Phytoplankton diversity and chemotaxonomy in contrasting North Pacific ecosystems

Antonija Matek [1], **Sunčica Bosak** [1], **Luka Šupraha** [2, 3], **Aimee Neeley** [4, 5], **Hrvoje Višić** [6], **Ivona Cetinić** [4, 7], **Zrinka Ljubešić** [Corresp. 1]

[1] Department of Biology, Faculty of Science, University of Zagreb, Zagreb, Croatia

[2] Department of Earth Sciences, Uppsala University, Uppsala, Sweden

[3] Section for Aquatic Biology and Toxicology (AQUA), Department of Biosciences, University of Oslo, Oslo, Norway

[4] Ocean Ecology Laboratory, NASA/Goddard Space Flight Center, Greenbelt, Maryland, United States

[5] Science Systems and Applications, Inc., Lanham, Maryland, United States of America

[6] Department of Geosciences, Faculty of Science, Eberhard Karls University Tübingen, Tübingen, Germany

[7] GESTAR II, Morgan State University, Baltimore, Maryland, United States

Corresponding Author: Zrinka Ljubešić
Email address: zrinka.ljubesic@biol.pmf.hr

Background. Phytoplankton is the base of majority of ocean ecosystems. It is responsible for half of the global primary production, and different phytoplankton taxa have a unique role in global biogeochemical cycles. In addition, phytoplankton abundance and diversity are highly susceptible to climate induced changes, hence monitoring of phytoplankton and its diversity is important and necessary.

Methods. Water samples for phytoplankton and photosynthetic pigment analyses were collected in boreal winter 2017, along transect in the North Pacific Subtropical Gyre (NPSG) and the California Current System (CCS). Phytoplankton community was analyzed using light and scanning electron microscopy and photosynthetic pigments by high-performance liquid chromatography. To describe distinct ecosystems, monthly average satellite data of MODIS Aqua Sea Surface temperature and Chlorophyll *a* concentration, as well as Apparent Visible Wavelength were used.

Results. A total of 207 taxa have been determined, mostly comprised of coccolithophores (35.5%), diatoms (25.2%) and dinoflagellates (19.5%) while cryptophytes, phytoflagellates and silicoflagellates were included in the group ''others'' (19.8%). Phytoplankton spatial distribution was distinct, indicating variable planktonic dispersal rates and specific adaptation to ecosystems. Dinoflagellates, and nano-scale coccolithophores dominated NPSG, while micro-scale diatoms, and cryptophytes prevailed in CCS. A clear split between CCS and NPSG is evident in dendogram visualising LINKTREE constrained binary divisive clustering analysis done on phytoplankton counts and pigment concentrations. Of all pigments determined, alloxanthin, zeaxanthin, divinyl chlorophyll *b* and lutein have highest correlation to phytoplankton counts.

Conclusion. Combining chemotaxonomy and microscopy is an optimal method to determine phytoplankton diversity on a large-scale transect. Distinct communities between the two contrasting ecosystems of North Pacific reveal phytoplankton groups specific adaptations to trophic state, and support the hypothesis of shift from micro- to nano-scale taxa due to sea surface temperatures rising, favoring stratification and oligotrophic conditions.

1   Phytoplankton diversity and chemotaxonomy in contrasting North

2   Pacific ecosystems

3   Antonija Matek [1], Sunčica Bosak [1], Luka Šupraha [2,3], Aimee Neeley[4,5] , Hrvoje Višić[6], Ivona

4   Cetinić [4,7], and Zrinka Ljubešić [1]

6   [1] Department of Biology, Faculty of Science, University of Zagreb, Zagreb, Croatia

7   [2] Department of Earth Sciences, Uppsala University, Uppsala, Sweden

8   [3] Section for Aquatic Biology and Toxicology, Department of Biosciences, University of Oslo,

9   Oslo, Norway

10   [4] Ocean Ecology Laboratory at NASA/Goddard Space Flight Center, Greenbelt, Maryland,

11   USA

12   [5] Science Systems and Applications, Inc., Lanham, MD, USA

13   [6] Department of Geosciences, Faculty of Science, Eberhard Karls University Tübingen,

14   Tübingen, Germany

15   [7] GESTAR II, Morgan State University, Baltimore, Maryland, USA

18   Corresponding Author:

19   Zrinka Ljubešić [1]

20   Email address: zrinka.ljubesic@biol.pmf.hr

Abstract

22 **Background.** Phytoplankton is the base of majority of ocean ecosystems. It is responsible for
23 half of the global primary production, and different phytoplankton taxa have a unique role in
24 global biogeochemical cycles. In addition, phytoplankton abundance and diversity are highly
25 susceptible to climate induced changes, hence monitoring of phytoplankton and its diversity is
26 important and necessary.

27 **Methods.** Water samples for phytoplankton and photosynthetic pigment analyses were
28 collected in boreal winter 2017, along transect in the North Pacific Subtropical Gyre (NPSG) and
29 the California Current System (CCS). Phytoplankton community was analyzed using light and
30 scanning electron microscopy and photosynthetic pigments by high-performance liquid
31 chromatography. To describe distinct ecosystems, monthly average satellite data of MODIS
32 Aqua Sea Surface temperature and Chlorophyll a concentration, as well as Apparent Visible
33 Wavelength were used.

34 **Results.** A total of 207 taxa have been determined, mostly comprised of coccolithophores
35 (35.5%), diatoms (25.2%) and dinoflagellates (19.5%) while cryptophytes, phytoflagellates and
36 silicoflagellates were included in the group ''others'' (19.8%). Phytoplankton spatial distribution
37 was distinct, indicating variable planktonic dispersal rates and specific adaptation to
38 ecosystems. Dinoflagellates, and nano-scale coccolithophores dominated NPSG, while micro-
39 scale diatoms, and cryptophytes prevailed in CCS. A clear split between CCS and NPSG is evident
40 in dendogram visualising LINKTREE constrained binary divisive clustering analysis done on
41 phytoplankton counts and pigment concentrations. Of all pigments determined, alloxanthin,
42 zeaxanthin, divinyl chlorophyll b and lutein have highest correlation to phytoplankton counts.

43 **Conclusion.** Combining chemotaxonomy and microscopy is an optimal method to determine
44 phytoplankton diversity on a large-scale transect. Distinct communities between the two
45 contrasting ecosystems of North Pacific reveal phytoplankton groups specific adaptations to
46 trophic state, and support the hypothesis of shift from micro- to nano-scale taxa due to sea
47 surface temperatures rising, favoring stratification and oligotrophic conditions.

Introduction

49 Phytoplankton have many important roles in the marine ecosystem: they are responsible for
50 half of the global primary production (Chavez, Messié & Pennington, 2011), contribute to the
51 biogeochemical cycles by being part of the biological pump through nutrient uptake and carbon
52 sequestration (Volk & Hoffert, 1985; Michaels & Silver, 1988; Karl & Church., 2017), and they
53 are at the base of majority ocean ecosystems (Pomeroy, 1974; Sherr & Sherr, 1991, Legendre &
54 Le Fèvre, 1995). Therefore, any changes in phytoplankton diversity impact the oceanic carbon
55 cycle, nutrient uptake, and zooplankton community structure, which has an indirect effect on
56 the whole oceanic ecosystem (Ramond et al., 2021). Consequences of global warming such as
57 temperature increase, change in ocean circulation and stratification, acidification, and
58 deoxygenation have an impact on the phytoplankton community (Rost, Zondervan & Wolf-

59   Gladrow, 2008). It is predicted that increases in ocean temperature and other climate induced
60   changes will affect phytoplankton metabolic rates and growth, ultimately changing the ocean-
61   wide phytoplankton diversity, and overall marine productivity (Moore et al., 2018; Cael,
62   Dutkiewicz & Henson, 2021). Due to this expected change in phytoplankton community in the
63   oceans of tomorrow, it is of extreme importance to understand the current oceanic
64   phytoplankton diversity and how it is shaped by environmental factors.

65   The North Pacific ecosystem is influenced by the Trade Winds, anticylonic North Pacific
66   Subtropical Gyre (NPSG), and the cyclonic Subarctic Gyre that bifurcate into California Current
67   System (CCS) and Alaska Current. The CCS is a transitional ecosystem that is more eutrophic in
68   comparison to NPSG because of the Columiba River's contributon of terrigenous sediments and
69   organic matter (Kammerer, 1987; Morgan, De Robertis & Zabel, 2005; Steele, Thorpe &
70   Turekian, 2008; Kudela et al., 2010; Capone & Hutchins, 2013; Catlett et al., 2021; Closset et al.,
71   2021; Abdala et al., 2022). Phytoplankton diversity of North Pacific was well recorded in
72   literature of 1970-1990s at one station, defined as CLIMAX area (28°N, 155°W) (Venrick, 1997).
73   The community was dominated by diatoms, then equally comprised of dinoflagellates, and
74   coccolithophorids, while cryptophytes, chryosphyceae, cyanobacteria and other groups
75   contributed less (Venrick, 1971; Venrick, 1982; Hayward, Venrick & McGowan, 1983; Venrick et
76   al., 1987; Venrick, 1990). Species number varied between 100 and 300, depending on number
77   of samples and ability to identify nano-fraction (Venrick, 1982; Venrick et al., 1987; Venrick,
78   1990). Recent research shows oligotrophic areas of North Pacific are usually dominated by pico-
79   and nanophytoplankton (Karl & Church., 2017; Kodama et al., 2021), while high community
80   diversity, with presence of larger microphytoplankton (e.g. diatoms) is found in eutrophic
81   regions of North Pacific (Du, Peterson & O'Higgins, 2015; Du & Peterson, 2018).

82   Large oceanic ecosystems, such as the North Pacific Ocean are showing response to changes in
83   climate (Venrick et al., 1987; Bograd et al., 2019; Litzow et al., 2020). For instance, in autumn of
84   2013, a warm blob appeared in the Gulf of Alaska, and by December of 2015, it expanded
85   toward Bering Sea, Transition Zone, and California Current System (CCS) (Peterson, Bond &
86   Robert, 2016). The blob-induced increase of the sea surface temperatures had an effect on
87   ecosystem, especially phytoplankton community structure across the whole north – east
88   Pacific. Phytoplankton community of oligotrophic NPSG shifted from nanophytoplankton to
89   picophytoplankton during warm phases of climate oscillations when stratification is strong, and
90   particle export is low (Yoon & Kim, 2020). Moreover, during the warm blob anomaly in the
91   eutrophic and diatom-dominated CCS, nutrient supply decreased for 50 % and the
92   phytoplankton community shifted to nonsiliceous phytoplankton and/or lightly silicified
93   diatoms (Closset et al., 2021). Long data records for North Pacific are collected at station
94   ALOHA (22.75°N, 158°W: A Long-term Oligotrophic Habitat Assessment) in NPSG (Karl &
95   Church., 2017) and Station M (34°50'N, 123°00'W; 4000 meters depth) in CCS ("Abyssal time-
96   series studies at Station M"). Three decades of data from ALOHA combined with improved
97   satellite algorithms are showing different trends of phytoplankton biomass, and net primary
98   production growth in response to positive phases of North Pacific Gyre Oscillation, Pacific

99   Decadal Oscillation and El Niño Southern Oscillation (Kavanaugh et al., 2018). Furthermore,
100   two-decade record on abyssal ecosystem at station M show strong benthic-pelagic cupling, and
101   significant response of the benthic communities to the climate induced changes in the ocean
102   surface ("Abyssal time-series studies at Station M"). All these studies demonstrate the
103   importance of time-series studies to record and predict future changes in ecosystems.

104   Recent advances in molecular and imaging technologies offer an unprecedented view of the
105   oceanic diversty (Gorocs et al., 2018; Shin et al., 2018; Fender et al., 2019; Hoving et al., 2019;
106   Fischer et al., 2020; Mirasbekov et al., 2021; Clayton et al., 2022). In a similar way,
107   chemotaxonomy offers the additional insight into the phytoplankton community structure and
108   direct connection with remote sensing (Kramer et al., 2022). However, our vision of the
109   phytoplankton diversity still relies on the morphological characterisation, usually done by
110   imaging. Image based taxonomy, although time consuming is by far the most wide-spread
111   method in determining phytoplankton community structure, in addition thanks to the new
112   automated instruments and technologies (Olson & Sosik, 2007; Picheral et al., 2010; Clayton et
113   al., 2022). Advances in imaging technology are contrasted by the decline in numbers of highly
114   trained taxonomic analysts as well as the new trainees entering the pipeline (Drew, 2011;
115   Pearson, Hamilton & Erwin, 2011; McQuatters-Gollop et al., 2017; Orr et al., 2021; Clayton et
116   al., 2022).

117   To fully understand the Pacific ecosystem, it is necessary to develop knowledge of the
118   phytoplankton diversity that relates to different ecosystems, changes in environment, and can
119   be used for future predictions of global warming's impact on marine ecosystems. Therefore, the
120   aim of this research was to represent a phytoplankton diversity of distinct trophic systems in
121   North Pacific using microscopy counts as main method, in combination with chemotaxonomy,
122   on a large spatial scale in a short period of time.

123   ## Materials & Methods

124   ### Expedition- location and time
125   Sea to Space Particle Investigation cruise aboard the Schmidt Ocean Institute R/V Falkor was
126   conducted from January 24 to February 20, 2017, in North Pacific (Fig. 1). The aim of the cruise
127   was to connect the radiometric properties (ocean colour) as well as ecological mechanisms of
128   carbon export (Durkin et al., 2022) with the trophic state of the ocean, and use those data to
129   develop algorithms and phytoplankton proxies for the NASA's PACE mission
130   (pace.oceansciences.org).

131   ### Sampling
132   Sampling was done along the investigated transect at Station 1 (ST1) and Station 2 (ST2) in
133   NPSG, and Station 3 (ST3) in CCS (Fig. 1). Each station represents a group of sampling sites
134   (Table 1) where CTD (conductivity, temperature, depth) casts were deployed at three depths:
135   the surface layer (S), deep chlorophyll maximum (DCM), and mixed layer depth (MLD), with
136   exception at CTD 14 where additional sample was taken below mixed layer depth (BMLD)

137   (Table 1). Due to the strong physical forcing, water column was well mixed as shown in CTD
138   profiles of all three stations in Durkin et al., 2022 (Supplemental Figure 1). Samples for
139   phytoplankton (n=38) and pigment analyses (n=38) were taken by 10 L Niskin rosette sampler
140   equipped with CTD and other sensors. For more detailed taxonomic analyses, additional
141   samples (n=38) were taken from the same Niskin bottles, and volume of 400 mL seawater was
142   filtered using weak vacuum onto 0.8 μm polycarbonate filters analyzed on SEM as described in
143   Šupraha, Ljubešić & Henderiks, 2018.

144   For qualitative plankton analysis, another set of samples (n=27) was taken from the Niskin
145   bottles and filtered through 20 μm mesh. Discrete phytoplankton and net phytoplankton
146   samples were fixed with 2% neutralized formaldehyde and stored in 250 mL bottles until
147   analyses in the laboratory of biological oceanography, Department of Biology, University of
148   Zagreb. Triplicate 4 L seawater samples were filtered on GF/F filters for phytoplankton pigment
149   analysis and stored in liquid nitrogen until the high-performance liquid chromatography (HPLC)
150   analysis in the NASA's Goddard Space Flight Center, following methods described in Hooker et
151   al., 2012.

152   Phytoplankton community analysis
153   Light microscopy (LM) was used to determine phytoplankton composition and abundance.
154   Subsamples of 50 or 100 mL, depending on cell density, were settled for 24 h and 48 h
155   respectively and analyzed under a Zeiss Axiovert 200 inverted microscope using the Utermöhl
156   method (Utermöhl, 1958) as described in Šupraha, Ljubešić & Henderiks, 2018. For additional
157   taxonomic analyses, net samples were analyzed with the Zeiss Axiovert 200 inverted
158   microscope and images of all species were taken and analyzed with Zeiss AxioVision SE64
159   (version 4.9.1). Micrograph plate of dominant taxa was made and edited using Adobe's
160   Photoshop CC 2015 and Illustrator CC 2017.

161   Phytoplankton are comprised of a phylogenetically diverse group of both prokaryotic and
162   eukaryotic organisms. Because of that, classification is much debated with different systematic
163   grouping (Bray & Curtis, 2006; Roy et al., 2011; Thomas et al., 2012; Pal & Choudhury, 2014).
164   Therefore, a simpler approach for classification will be presented in this paper with focus on
165   morphological characteristics of most abundant forms only: cyanobacteria, diatoms,
166   dinoflagellates, coccolithophores, cryptophytes and "others" – including phytoflagellates,
167   silicoflagellates, ciliates and other genera. Phytoplankton were classified on size variation using
168   the equivalent spherical diameter (ESD) of cells as nanophytoplankton (ESD 2–20 μm) and
169   microphytoplankton (ESD 20–200 μm).

170   Trophic indices and spatial distribution
171   Pigment average concentrations were calculated in order to get F_p index using formula by
172   Claustre, 1994: F_p = (sum of average concentrations of fucoxanthin and peridinin) / (sum of
173   average concentrations of all primary pigments). Spatial distribution across investigated
174   transects was visualized by creating one chart showing abundances of phytoplankton groups,

175   and another one with distribution of the subset of pigments that best correlate to
176   phytoplankton community (the correlation test explained later in Statistical analysis section).
177   Chart plotting and calculations were made using the software Grapher 12 (GoldenSoftware)
178   and Microsoft Office 365 ProPlus (Microsoft Corporation, version 1705), respectively.

179   ## Satellite data
180   To illustrate distinct trophical ecosystem-specific properties of investigated area, monthly
181   average satellite data (February 2017) of MODIS Aqua Sea Surface temperature and Chlorophyll
182   *a* concentration, as well as Apparent Visible Wavelength (AVW) was used. AVW is an optical
183   water type classification that allows for a single, highly sensitive metric to combine the
184   information about the spectral shape of the ocean colour (Vandermeulen et al., 2020), where
185   spectral shift in AVW indicates changes in oceanic components contribution to the ocean color.
186   In open ocean, ocean colour is driven by the phytoplankton community and associated detrital
187   component, and in coastal ocean dissolved organic matter and sediment can contribute as well.
188   As such, it is a great geophysical tool to evaluate spatial and temporal changes across oceanic
189   ecosystems.

190   ## Statistical analysis
191   Several statistical analyses were done using Primer 7.0. (Primer-E Ltd 2021) to test similarities
192   between ST1, ST2 and ST3, and correlation between phytoplankton counts and pigment data in
193   order to gain better understanding of community diversity.

194   ### Analysis of similarity
195   Bray–Curtis (BC) rank similarity matrix was calculated using log(x+1) transformed data (Bray &
196   Curtis, 2006) of phytoplankton counts. To test significance of similarity between ST1, ST2, and
197   ST3, we run pairwise analysis of similarity (ANSOIM R statistic) on BC rank similarity matrix. Test
198   takes averages of ranks within matrix and calculates their differences within each group in the
199   cluster (Clarke et al., 2014). Furthermore, similarity percentages analyses (SIMPER) (Clarke,
200   1993) were used to observe the percentage contribution of each taxon to the average
201   dissimilarity between samples of different groups (ST1, ST2, and ST3).

202   ### Correlation tests
203   In addition, another BC rank similarity matrix was calculated on log(x+1) transformed data of
204   pigment concentrations at ST1, ST2, and ST3. We run RELATE analysis, BEST global test, and
205   LINKTREE analyses using both BC matrices in order to test if there is a significant correlation
206   between pigment concentrations and phytoplankton counts data.

207   RELATE statistic with Spearman correlation method shows how well two similarity matrices
208   relate to each other by calculating correlation factor (Clarke et al., 2014). The analysis was done
209   on BC rank similarity matrix of pigments concentrations and BC matrix of phytoplankton counts.
210   In case RELATE analysis indicate a high correlation factor, BEST global test is run to find the
211   subset data of one BC matrix (in our case pigment concentrations) that explains the structure of
212   data in another BC matrix (in our case phytoplankton counts) (Clarke et al., 2014). In that way

213 we aim to calculate which set of pigments have the highest correlation with the phytoplankton
214 community structure.

215 In order to visualize the correlation between resulted pigment set and phytoplankton counts,
216 and test its significance, LINKTREE constrained binary divisive clustering analysis and similarity
217 profile test (SIMPROF) were run, respectively (Clarke et al., 2014). LINKTREE produces a
218 dendrogram that shows clustering of ST1, ST2, and ST3 based on phytoplankton counts, and at
219 the same time explains the cluster structure by showing which pigment concentration
220 thresholds cause the main splits.

221 Results

222 North Pacific ecosystem and water column hydrography

223 Satellite data monthly averaged for February 2017 confirm ST1, ST2 (NPSG), and ST3 (CCS) are
224 located in distinct ecosystems (Fig. 1). NPSG has higher sea surface temperature compared to
225 CCS (MODIS Aqua Sea Surface temperature data, Fig. 1a), where Chl *a* concentration is much
226 higher (MODIS Aqua Chlorophyll *a* concentration data, Fig. 1b). Furthermore, MODIS Aqua
227 Apparent Visible Wavelength data (Fig. 1c) indicates differences between two sampled
228 environments based on the spectral shape of the color of the ocean: eutrophic CCS (higher
229 AVW) and oligotrophic NPSG (lower AVW).

230 The deep chlorophyll maximum layer (DCM) was defined as highest fluorescence signal
231 encountered during station profiles. For profiles collected at ST1 and ST2, it set at ~130 m,
232 while it was found at much shallower depths at coastal ST3 (~30 m). As expected mixed-layer
233 depth (MLD, calculated as the depth at which density differed from the mean density in the top
234 10 m by < 0.05 kg m^{-3}), was sitting in proximity of the DCM, at ~ 130 m for ST1 and ST2, and at ~
235 90 m depth at ST3.

236 Phytoplankton diversity of North Pacific Ocean

237 The encountered phytoplankton community was mostly comprised of coccolithophores
238 (35.5%), diatoms (25.2%) and dinoflagellates (19.5%) while cryptophytes, phytoflagellates and
239 silicoflagellates, etc. were included in group "other" that makes 19.8% of phytoplankton counts.
240 A total of 207 taxa have been determined from both Niskin and net samples of which: 106
241 diatoms, 48 coccolithophores, 41 dinoflagellates, 7 other autotrophs, 4 heterotrophs, and 1
242 cyanobacterium. Cryptophytes were observed but were not identified to the genus level (Table
243 S1). Of the 207 taxa, more than a half (113) taxa are found only in net samples: 42 diatoms, 40
244 coccolithophores, 27 dinoflagellates and 4 other heterotrophs.

245 Spatial distribution of phytoplankton groups using microscopy and pigments

246 Microscopy counts resulted in abundances of phytoplankton groups that indicate lower
247 biomass of micro- and nanophytoplankton at NPSG oligotrophic ecosystem (ST1 and ST2) in
248 comparison to eutrophic CCS (ST3). Moreover, results elucidate variable spatial distribution of
249 microphytoplankton, while spatial distribution of nanophytoplankton is even (Fig. 2a and 2b).

250   Diatoms of micro-fraction increased for an order of magnitude with the transition to ST3, while
251   distribution of dinoflagellates, coccolitophores, and other phytoplankton groups of
252   microphytoplankton stay constant across the investigated transect (Fig. 2a). Nano fraction of
253   diatoms, dinoflagellates, and coccolitophores had even distribution across stations, while
254   "other" cells (e.g. cryptophytes) exhibited similar behaviour to micro-scale diatoms, increasing
255   their abundances at ST3 (Fig. 2b).

256   Average pigment concentrations encountered on transect (Table S4) show F_p index that is
257   higher at ST3 (0,087), and lower at ST1 (0,018) and ST2 (0,021). Alloxanthin, zeaxanthin, divinyl
258   chlorophyll *b* (DVChl *b*), and lutein are the pigment set with the highest correlation to
259   phytoplankton counts, as identified by the BEST global test that resulted in Spearman
260   correlation coefficient (Rho=0.532) with $p < 0.1\%$ significance level (Table S3). Spatial
261   distribution of these four pigments and divinyl chlorophyll *a* (DVChl *a*) across stations elucidates
262   two clearly distinct environments (Fig. 3a). ST1 and ST2 exhibited higher concentrations of
263   DVChl *a*, and zeaxanthin, the biomarkers for *Prochlorococcus* and *Synechococcus* (respectively),
264   implying the cyanobacteria domination in this region. Entering ST3, concentrations of previous
265   pigments fall substantially, while concentrations of cryptophytic biomarker alloxanthin rise.
266   Moreover, we observed higher concentrations of 19'-hexanoyloxyfucoxanthin (19HF) and
267   fucoxanthin (Table S4), biomarkers for coccolithophores and mostly diatoms, respectively.
268   Biomarkers peridinin and prasinoaxanthin also dominated at ST3, representing high
269   abundances of dinoflagellates and prasinophytes, respectively (Table S4). Furthermore, there is
270   a strong increase of total Chl *a* concentration at ST3, when compared to oligotrophic ST1 and
271   ST2 (Fig. 3b).

272   ## Similarity between stations and dominant taxa
273   Pairwise test of ANOSIM analysis displayed significant differences in phytoplankton community
274   abundance and composition between ST1 and ST3, and ST2 and ST3 with R-value being 0.579
275   and 0.612, respectively (Table S2). Taxa diversity and abundances were largest at eutrophic ST3,
276   while oligotrophic ST1 and ST2 exhibited similar community structure.

277   Nano-scale dinoflagellates and coccolithophores contributed the most to dissimilarity of both
278   ST1 and ST2 according to SIMPER analysis results (Table 2). Next were phytoflagellates with
279   high contribution to the ST1 dissimilarity, while at ST2 that was *Rhizosolenia hebetata f.*
280   *semispina* (Table 2). Nano-scale coccolitophorids (ESC 5-10 µm), cryptophytes and *Pseudo-*
281   *nitzschia pseudodelicatissima* contributed the most to dissimilarity of ST3 (Table 2).

282   Dominant taxa by stations were defined as species and groups with abundance $>10^4$ cells L^{-1},
283   and the frequency of occurrence in samples >50 % (Table 3), and some of them are shown on
284   micrographs (Figure 4). Dominant taxa present along the whole transect, but reaching highest
285   abundances at ST3 were cryptophytes, *Gyrodinium spp*, *Nitzschia bicapitata*, nano-
286   dinoflagellates and nano-coccolithophores (ESC <10 µm) (Table 3). On the other hand, some
287   dominant taxa were present at only one station. Species specific to ST1 were nano-scale

288 *Gyrodinium* sp*.* (ESC <20 μm), *Gymnodinium* spp., *Michaelsarsia adriaticus, N. braarudii*, and
289 *Nitzschia* sp. Specific taxa at ST2 were *Calciosolenia brasiliensis, Nitzschia* sp., *Ophiaster sp.*, and
290 nano-coccolithophores (ESC 10-20 μm). The highest number of specific species was found at
291 ST3, and most of them were diatoms: *Chaetoceros contortus, Ch. convolutus, Ch. debilis,*
292 *Lennoxia faveolata, N. sicula, Proboscia alata, Pseudo-nitzschia pseudodelicatissima, R.*
293 *hebetata f. semispina, R. cleveii, Thalassionema nitzschioides*, and nano-scale *Thalassiosira* sp.
294 (ESC <20 μm). Other two specific taxa for ST3 were *Micromonas* sp. and *Oxytoxum cf. variabile*
295 (ESC <20 μm) (Table 2). Highest abundance of diatoms at ST3 was recorded thanks to the high
296 quantities of *Pseudo-nitzschia pseudodelicatissima*.

Correlation between pigments and phytoplankton counts

298 HPLC based pigment concentrations closely followed the significant across-transect trends
299 observed in phytoplankton abundances, as demonstrated by the RELATE test (Fig. S1b).
300 Alloxanthin, zeaxanthin, DVChl *b*, and lutein contributed the most to similarities in trends, as
301 shown by the BEST global test (Table S3). A clear split between coastal, eutrophic ST3 and
302 oligotrophic ST1 and ST2 is visible in dendogram visualising LINKTREE constrained binary
303 divisive clustering analysis done on phytoplankton counts and pigment concentrations (Fig. 5).
304 This primary split (Node A>B, K), that can be explained by the specific threshold of alloxanthin (-
305 0.0089 μg/L for ST1 and ST2, 0,001 μg/L for ST3) is highly significant (SIMPROF test, Fig. S1a).

306 Further splits in the dendogram are driven by secondary pigments and demonstrate finer
307 differences within the ecosystem types, on oligotrophic side lutein or zeaxantin (Node B), and
308 on eutrophic side by zeaxantin (Node K>L, N) and further down (Node N) by the lutein. Note
309 that only some of the splits in this dendogram are significant (black lines on the Fig. 5)
310 according to SIMPROF test (Fig. S1a).

Discussion

Horizontal distribution of phytoplankton

313 Planktonic dispersal rate varies across marine planktonic taxa, while negative relationship
314 between dispersal scale and body size causes less abundant and larger-fraction plankton (in
315 near-surface, epipelagic waters) to have shorter dispersal scales and larger spatial species-
316 turnover rates than the more abundant, smaller-fraction plankton (Villarino et al., 2018). The
317 larger phytoplankton will be more similar at geographically proximate locations, and dissimilar
318 between distant locations while it would allow smaller, more abundant phytoplankton (body
319 size <2 mm) to travel greater distances (Finlay, 2002; Martiny et al., 2006; Villarino et al., 2018).
320 This explains even spatial distribution of all nanophytoplankton fractions between stations,
321 while microphytoplankton fractions, especially diatoms, are most abundant at ST3 (Fig. 3a and
322 b). Additionally, we observed the highest number of specific diatom species at ST3 (Table 2).

Phytoplankton community structure

324 Phytoplankton community of North Pacific comprised of 207 taxa, of which most abundant
325 were coccolithophores (35.5%), then diatoms (25.2%), dinoflagellates (19.5%) and others

326 (19.8%) including cryptophytes, phytoflagellates, and silicoflagellates. Microphytoplankton was
327 more abundant at eutrophic ST3, with diatoms being dominant taxa while oligotrophic ST2 and
328 ST1 were dominated by nano-scale coccolithophores and dinoflagellates, which is supported by
329 molecular data obtained from the same cruise shown in Durkin et al., 2022. Proportion of taxa
330 read abundances in exported ASVs (Amplicon sequence variants) was distinct between ST2 and
331 ST3, with higher diatom read abundances at ST3 (78%), and lower at ST2 (10%), and small
332 proportion of cryptophyta and haptophyta reads at ST3 (15%), and large contribution at ST2
333 (49%) (Durkin et al., 2022).

334 Microphytoplankton
335 Microphytoplankton abundance increased at eutrophic ST3 (Fig. 2a), where diatoms were
336 dominant (Table 3) and contributed the most to the dissimilarity to other stations (Table 2).
337 Similar assemblage was discussed in a study done by Iriarte & Fryxell, 1995 who researched
338 microphytoplankton community structure at equatorial Pacific at 140°W during El Niño 1992
339 event. Taxa groups that contributed the most to the biomass were diatoms, dinoflagellates and
340 coccolitophores. Dominant species during March to April were *Pseudo-nitzschia delicatissima*,
341 *Thalassionema* spp., *Thalassiothrix* spp., *Thalassiosira lineata*, and *Oxytoxum variabile*. In
342 October the same species dominated, with additional two: *Calcidiscus leptoporus* and
343 *Chaetoceros atlanticus*. Furthermore, Yamaguchi et al., 2002 analyzed plankton of three regions
344 in western North Pacific: subarctic, subtropical and transitional. Eutrophic subarctic region had
345 the highest phytoplankton biomass, and community dominated with dinoflagellates and
346 diatoms. During North Pacific cruise along 155°W in January 1966, diversity of diatoms was
347 analyzed using light microscopy, and 54 species were identified, of which 37 were frequent
348 (Venrick, 1971). Dominant diatoms were *Chaetoceros atlanticus*, *Ch. peruvianus*, *Denticula*
349 *seminae*, *Nitzschia lineola*, *Thalassiothrix longissima*, and *Pleurosigma normanii* (Venrick, 1971).
350 Moreover, analyses of time series database including 12-year record of phytoplankton
351 abundances, yielded list of dominant species comparable to ours: *N. bicapitata*, *N. braarudii*, *N.*
352 *sicula, Pseudo-nitzschia pseudodelicatissima., Thalassionema sp,.and Oxytoxum cf. variabile*
353 (Venrick, 1990). A recent molecular study on diatom assemblages in CCS revealed species with
354 highest relative abundance of reads: *Rhizosolenia* sp., *Actinocyclus* sp., *Thalassiosira*
355 *diporocyclus*, *Asteromphalus* sp., and *Fragilariopsis doliolus* (Abdala et al., 2022).
356
357 Eutrophic ST3 had the highest abundances of *Pseudo-nitzschia pseudodelicatissima* that was
358 absent from ST1 and ST2. *Pseudonitzschia* taxa, while cosmopolitant (Hasle, 2002), seems to be
359 prevalent in communities along the California coast, where it has been recorded since 1930s
360 (Gran & Thompson, 1930). The appearance of these species coincided with upwelling zones
361 near the coast (Trainer et al., 1998), while others point to areas with increased fertilizer use and
362 agricultural run-off causing eutrophication (Smith et al., 1990). *Pseudo-nitzschia* species are
363 known to respond to the environmental drivers - both human induced and those specific for
364 ecosystem (Parsons & Dortch, 2002), and increased molecular and taxonomy analyses yielded
365 more knowledge on their ecology, physiology, phylogeny and distribution (Trainer et al., 2012).
366 Species recorded in CCS often causing toxic blooms are *P. australis* and *P.multiseries*, while *P.*
367 *pseudodelicatissima* was frequent along Washington coast (Trainer et al., 2012). A diatom

368   species *Lennoxia faveolata* had the second-highest abundance among diatoms at ST3 and was
369   not detected in other stations. Thomsen et al., 1993 who first described it, found high numbers
370   in samples from Californian waters during winter, but not much more is known about it.

371   Nanophytoplankton
372   Horizontal distribution of nano-fraction was even among stations, while cryptophytes
373   abundance increased in eutrophic CCS (Fig. 2b). Molecular analyses by Durkin et al., 2022
374   confirms this distribution, showing high relative proportion of nano-scale dinoflagellate reads in
375   exported ASVs at both ST2 and ST3 (67% and 78%, repsectively), and high cryptophyta read
376   abundances at ST3 (49%). Furthermore, our results show cryptophytes, coccolithophorids and
377   dinoflagellates dominated entire investigating area (Table 3), and the latter two contributed the
378   most to the dissimilarity of both ST1 and ST2 (Table 2). Similarly, Taylor & Landry, 2018
379   combined epifluorescence microscopy and flow cytometry to assess diversity of North Pacific
380   showing oligotrophic NPSG, and eutrophic CCS are dominated by nanophytoplankton, and
381   micro-scale diatoms, respectively.

382   Coccolithophores
383   Coccolithophorid contribution to community composition is significant on all stations, with
384   dominant nano- fraction, especially at greater depths. Micro-scale coccolithophores have a
385   more significant abundance at ST1 and ST2, but they are absent at ST3. Coccolithophorid
386   pigment proxy 19HF has a relatively high ratio on all stations when compared to other
387   pigments. Its presence may point to the higher contribution of pico-scale coccolithophores in
388   bigger depths at ST3. *Michaelsarsia adriaticus* was a dominant species present only at ST1,
389   whereas dominant *Calciosolenia brasiliensis* and *Ophiaster* sp. were specific to ST2. Dominant
390   species observed on both ST1 and ST2 were *C. murrayi* and *Discosphaera tubifera*. ST3 was
391   dominated by nano-scale coccolithophorids (ESC <5 µm and 5-10).

392   Domination of coccolithophores at ST1 and ST2 point to species more adapted to oligotrophic
393   conditions, while indirect observation of 19HF at ST3 implies a shift to the more eutrophic-
394   adapted, smaller coccolithophores species. Li et al., 2013 observed concentrations of 19HF in
395   the Pacific that was low in the upper euphotic zone but increased with depth. Fujiki et al., 2016
396   also observed low surface 19HF and 19BF concentration (< 0.5 mg/m^3) that is increasing below
397   70 m. This would suggest that the coccolithophores are physiologically adapted to low light,
398   nutrient-enriched regions of the water or the 19HF came from other lineages containing the
399   coccolithophorid-indicative marker pigment (Carreto et al., 2001; Landry, 2003).

400   Okada & Honjo, 1973 recorded 90 coccolithophorid species in North and Central Pacific. Based
401   on community structure, they described 6 zones, and Zones B (Transitional Pacific) and C
402   (Central-North Pacific) match our sampling transect. They observed high abundance of
403   *Emiliania huxley* (cold variety), *Rhabdosphaera clavigera*, and *Umbellosphaera irregularis*. Less
404   abundant species present in this area were *Discosphaera tubifera*, *Syracosphaera* spp, *R.*
405   *stylifera*, *U. tenuis*, *Umbilicosphaera hulburtiana*, *U. sibogae*, which is similar community
406   structure observed in our study (Table S1), however we observed other dominant species:

407   *Calciosolenia brasiliensis, C. murrayi, D. tubifera, Michaelsarsia adriaticus*, and *Ophiaster* sp
408   (Table 3). Hoepffner & Haas, 1990 identified nanophytoplankton community of NPSG by using
409   electron microscopy, and observed that Prymnesophyceae contributed the most (55%), with
410   equal abundances of Prymnesiales and Coccosphaerales. Dominant taxa were *E.huxley, O.*
411   *formosu*s, *R. clavigera*, and *C. murrayi*. Another study in NPSG revealed a total of 53 species,
412   from which most abundant were *D. tubifera, U. tenuis*, and *Heladosphaera cornifera* in the
413   upper layer (0 -80 m), and *Anthosphaera oryza, Florisphaera profunda, Thorosphaera flabellata*,
414   and *Oolithotus fragilis* in the lower layers (140-200 m) (Reid, 1980). Other frequent species
415   observed at the surface were *Acanthoica acanthifera, Calyptrosphaera oblonga, U. irregularis,*
416   *R. stylifera, S. pulchra*, and *S. pirus* (Reid, 1980). Most of listed species we detected as well
417   (Table 3).

418   Cyanobacteria
419   In general, *Synechoccocus* is more ubiquitous (Campbell & Vaulot, 1993; Li, 1995; Blanchot &
420   M, 1996; Otero, Álvarez-Salgado & Bode, 2020), and often more abundant in colder and
421   nutrient-richer coastal waters (Biller et al., 2014), whereas *Prochlorococcus* prefers warm
422   oligotrophic waters with temperatures >15 °C (Partensky, Blanchot & Vaulot, 1999b), and its
423   abundance drops above 50°N (Partensky, Hess & Vaulot, 1999a). Temperature and
424   environmental hydrodynamics may influence variation in the abundances, structure, and
425   distribution of both *Prochlorococcus* and *Synechococcus* populations, making them ideal
426   indicator organisms for predicting future changes in the ecosystems caused by the global
427   warming (Babić et al., 2017).

428   Pigments DVChl *a*, and zeaxanthin, biomarkers of cyanobacteria *Prochlorococcus* and
429   *Synechococcus*, respectively, were recorded in high concentration at oligotrophic NPSG (ST1
430   and ST2), that falls substantially towards eutrophic CCS (ST3). Zeaxanthin concentrations were
431   less variable throughout investigated transect (Table S4, Fig. 3a). Therefore, our results imply
432   high abundance of *Prochlorococcus* and *Synechococcus* at oligotrophic NPSG, with
433   *Synechococcous* being more adapted to eutrophic ecosystem, which was also confirmed in a
434   study done by Taylor & Landry, 2018.

435   Another research done during Sea to Space Particle Investigation cruise yielded results on the
436   inorganic carbon fixation rates, and nitrate, ammonium, and urea uptake rate at the single cell
437   level in photosynthetic picoeukaryotes (PPE), *Prochlorococcus* and *Synechococcus* (Berthelot et
438   al., 2019). The flow cytometry was used, elucidating high abundance of *Prochlorococcus* at
439   NPSG, and better adaptation of *Synechococcus* to eutrophic CCS region (Berthelot et al., 2019).
440   Other studies done in oligotrophic regions of the North Pacific also observed dominance of
441   *Prochlorococcus*, followed by high abundance of *Synechococcus* (Andersen et al., 1996; Fujiki et
442   al., 2016). These results can be explained with taxa-specific physiological and photosynthetic
443   adaptation to different biogeochemical conditions of the two ecosystems (Partensky, Hess &
444   Vaulot, 1999a; Partensky, Blanchot & Vaulot, 1999b; Biller et al., 2014).

445 *Synechococcus* may also be indirectly observed using the abundance of diatom *Leptocylindrus*
446 *mediterraneus* because it has a symbiont colonial protozoan *Solenicola setigera* Pavillard inside
447 which the *Synechococcus* may reside (Buck & Bentham, 1998; Gómez, 2007). *Leptocylindrus*
448 *mediterraneus* has been detected on both the ST1 and ST2, albeit with low abundance.
449 Nevertheless, the number of cyanobacterial cells should be much higher than the number of
450 symbionts they inhabit. Therefore, although we already detected cyanobacteria by using HPLC
451 pigment analysis, it could be possible to use this indirect three-partner associated symbiosis as
452 a method to record the presence of *Synechococcus*.

453 ## Phytoplankton chemotaxonomy and its relation to microscopy
454 Chemotaxonomy is a method that allows characterization of the phytoplankton community to
455 coarser taxa than the microscopy can, however, offering insight into the nano- and pico-
456 planktonic composition that is undetectable by classical microscopy methods (Kramer, Siegel &
457 Graff, 2020). Following the decades of research in which pigment composition was related to
458 the microscopy based one, it proved to have biases as concentrations of pigment biomarkers,
459 and their relation to the chlorophyll *a* are not always the best representative of the targeted
460 taxa (Harry Havskum et al., 2004; Irigoien et al., 2004; Pan et al., 2020). These vary with
461 physiology of the cells, and environmental factors such as irradiance, nutrient availability, day
462 length, temperature, and mixing status (Higgins, Wright & Schluter, 2011).

463 Regardless of biases, HPLC approach allowed us to track distribution of cyanobacterial taxa
464 indirectly through their pigments proxy, DVChl *a*, and zeaxanthin, that reached their highest
465 peak at oligotrophic ST1 and ST2. Highest concentrations of fucoxanthin, peridinin, 19HF,
466 alloxanthin, and prasinoxanthin were observed at ST3 (Table S4), which indicate higher
467 abundances of diatoms, dinoflagellates, coccolitophores, cryptophytes, and prasinophytes
468 respectively. Similarly, chemotaxonomy analyses of subsurface chlorophyll maximum (SCM) at
469 western Baja California also showed dominance of diatoms, prasinophytes, and cryptophytes,
470 in addition to haptophytes, pelagophytes, and picocyanobacteria (Almazán-Becerril, Rivas &
471 García-Mendoza, 2012). Recent HPLC 22-year time series data on CCS phytoplankton
472 community confirms significant contribution of diatoms, followed by dinoflagellates,
473 chlorophytes, prymnesiophytes, and picophytoplankton (Catlett et al., 2021). Furthermore, one
474 interesting trend arose from LINKTREE statistical analysis, showing that pigment alloxanthin
475 determined most the differences in phytoplankton community between the CCS and open
476 ocean stations (Fig. 5). While the imaging-based analysis did point cryptophytes play an
477 important role in distinguishing two communities (Table 2), other taxa, namely
478 coccolithophorids and diatoms also seemed to drive the ecosystem differences.

479 Claustre, 1994 proposed another use of pigments that can determine trophic state of the area
480 by calculating the F_p index (the ratio of pigments highly correlated to changes in Chl *a*
481 concentration to other pigments that are less variable). Study showed fucoxanthin and
482 peridinin, biomarkers for mostly diatoms and dinoflagellates respectively, had a higher
483 correlation with the change of total Chl *a* in comparison to other pigments, meaning rise in

484   biomass can be correlated with diatoms and dinoflagellates growth. We used the same
485   approach and calculated higher F_p index at ST3 in comparison to ST1 and ST2, which correlates
486   with the rise of fucoxanthin and peridinin in CCS (Table S4).

487   **Contrasting North Pacific ecosystems**

488   In this paper, the analyzed data showed distinct environments characterized by differences
489   between phytoplankton abundances and concentrations of pigments along a transect that
490   comprises an open ocean and a coast. We recorded lower phytoplankton counts at NPSG which
491   is the largest ecosystem on the planet with reduced intake of nutrients in the euphotic zone,
492   low primary production (PP) and export of carbon to deeper layers (Karl & Church., 2017;
493   Kavanaugh et al., 2018). On the other hand, the phytoplankton counts were higher at the CCS
494   that is more eutrophic ecosystem with seasonal upwellings, higher PP, and frequent blooms
495   ("Abyssal time-series studies at Station M"; Closset et al., 2021). Furthermore, the Columbia
496   River influences the CCS with an increased terrigenous contribution raising the trophic state
497   (Hickey & Banas, 2008). Differences between ecosystems can also be detected by observing
498   maximum chlorophyll *a* concentration, and our results show that it was higher and more
499   variable in CCS, in comparison to NPSG. High chlorophyll *a* concentrations were already
500   recorded in northern part of CCS (Ware & Thomson, 2005), while studies in other eutrophic
501   ecosystems show similar trend (Zhang, Wang & Yin, 2018; Miranda-Alvarez et al., 2020). Fujiki
502   et al., 2016 observed low Chl *a* concentration at the ALOHA station (< 0.05 mg/m^3), whereas at
503   ST1 and ST2 concentration did not exceed 0.4 µg/L.

504   ## Conclusions
505   Our results demonstrate the power of combined techniques, in this case microscopy and
506   pigments, when exploring the ecosystem diversity (Irigoien et al., 2004). We optimized the
507   method for analyzing phytoplankton diversity on a large-scale transect , so with both
508   techniques separately managed to independently differentiating two contrasting ecosystems.
509   Furthermore, each of the techniques, thanks to their strengths and biases, defined different
510   taxonomic drivers. Dominant group revealed by light microscopy were diatoms, with most
511   abundant species being *Pseudo-nitzschia pseudodelicatissima.* SEM results show
512   cococclithophorids species dominated nanophytoplankton, and their community shifted from
513   large species in NPSG to smaller in CCS. All biomarker signature pigments correlated with
514   taxonomic groups, revealing higher abundance of cyanobacteria in oligotrophic NPSG
515   ecosystem, however *Synechococcus* was better adapted to eutrophic CCS in comparison to
516   *Prochlorococcus*. Cryptophytes were recognized as group with important role in distinguishing
517   between the CCS and NPGS phytoplankton communities, which was confirmed both by pigment
518   and imaging-based analysis. Alloxanthin, zeaxanthin, divinyl chlorophyll *b*, and lutein were the
519   most important when it comes to distinguishing the community composition across the
520   investigated transect. However, they were not connected to dominating microflora, but to "less
521   charismatic" and elusive microscopy nano- and pico-scale plankton, such as cryptophytes,
522   prasinophytes, and *Prochlorococcus*. Phytoplankton distinct spatial distribution along the

523 investigated transect indicates variable planktonic dispersal rates and specific adaptations to
524 different trophic ecosystems. Furthermore, observed trends supports findings of other studies
525 indicating a global shift from micro- to nano-scale phytoplankton due to climate-change
526 induced sea surface temperatures rising, causing water layer stratification and oligotrophic
527 environment conditions (Litchman et al., 2007; Finkel et al., 2007; Winder & Sommer, 2012;
528 Yoon & Kim, 2020; Benedetti et al., 2021; Closset et al., 2021). As we are moving towards an era
529 where we will be able to observe global phytoplankton diversity from space (e.g. NASA PACE
530 mission) (Werdell et al., 2019), studies such as these give us an important insight in how
531 different taxonomic approaches (that are used to validate remote sensing algorithms) offer a
532 different views of the changing ocean.

533 **Funding:** This work was funded by Croatian Science Foundation under projects BIOTA (UIP-
534 2013-11-6433) and ISLAND (IP-2020-02-9524), the Schmidt Ocean Institute, NASA GSFC Ocean
535 Ecology Lab, and NASA's PACE mission. We thank Jorijntje Henderiks for providing financial
536 support for SEM analyses at Uppsala University (Swedish Research Council grant 2011-4866 and
537 other funding).

538 **Acknowledgments:** We thank the captain and crew of the R/V Falkor and the "Sea to Space"
539 science party, who made this research possible.

540 References

541 Abdala ZM, Clayton S, Einarsson SV, Powell K, Till CP, Coale TH, Chappell PD. 2022. Examining

542 ecological succession of diatoms in California Current System cyclonic mesoscale eddies.

543 *Limnology and Oceanography* n/a:1–17. DOI: 10.1002/lno.12224.

544 Abyssal time-series studies at Station M. *Available at https://www.mbari.org/station-m-time-*

545 *series/* (accessed December 1, 2022).

546 Almazán-Becerril A, Rivas D, García-Mendoza E. 2012. The influence of mesoscale physical

547 structures in the phytoplankton taxonomic composition of the subsurface chlorophyll

548 maximum off western Baja California. *Deep Sea Research Part I: Oceanographic*

549 *Research Papers* 70:91–102. DOI: 10.1016/j.dsr.2012.10.002.

550 Andersen RA, Bidigare RR, Keller MD, Latasa M. 1996. A comparison of HPLC pigment signatures

551 and electron microscopic observations for oligotrophic waters of the North Atlantic and

552   Pacific Oceans. *Deep Sea Research Part II: Topical Studies in Oceanography* 43:517–537.

553   DOI: 10.1016/0967-0645(95)00095-X.

554 Babić I, Petrić I, Bosak S, Mihanović H, Radić ID, Ljubešić Z. 2017. Distribution and diversity of

555   marine picocyanobacteria community: Targeting of Prochlorococcus ecotypes in winter

556   conditions (southern Adriatic Sea). *Mar. Genomics* 36:3–11. DOI:

557   10.1016/j.margen.2017.05.014.

558 Benedetti F, Vogt M, Elizondo UH, Righetti D, Zimmermann NE, Gruber N. 2021. Major

559   restructuring of marine plankton assemblages under global warming. *Nature*

560   *Communications* 12:5226. DOI: 10.1038/s41467-021-25385-x.

561 Berthelot H, Duhamel S, L'Helguen S, Maguer J-F, Wang S, Cetinić I, Cassar N. 2019. NanoSIMS

562   single cell analyses reveal the contrasting nitrogen sources for small phytoplankton. *The*

563   *ISME Journal* 13:651–662. DOI: 10.1038/s41396-018-0285-8.

564 Biller S, Berube P, Berta-Thompson J, Kelly L, Roggensack SE, Awad L, Roache-Johnson KH, Ding

565   H, Giovannoni SJ, Rocap G, Moore LR, Chisholm SW. 2014. Genomes of diverse isolates

566   of the marine cyanobacterium Prochlorococcus. *Sci Data* 1:140034. DOI:

567   10.1038/sdata.2014.34.

568 Blanchot J, M R. 1996. Picophytoplankton abundance and biomass in the western tropical

569   Pacific Ocean during the 1992 El Nino year: Results from flow cytometry. *Deep. Res. Part*

570   *I Oceanogr. Res. Pap* 43:877–895. DOI: 10.1016/0967-0637(96)00026-X.

571 Bograd SJ, Kang S, Di Lorenzo E, Horii T, Katugin ON, King JR, Lobanov VB, Makino M, Na G,

572   Perry RI, Qiao F, Rykaczewski RR, Saito H, Therriault TW, Yoo S, Batchelder H. 2019.

573   Developing a Social-Ecological-Environmental System Framework to Address Climate

574 Change Impacts in the North Pacific. *Frontiers in Marine Science* 6:333. DOI:

575 10.3389/fmars.2019.00333.

576 Bray JR, Curtis JT. 2006. An Ordination of the Upland Forest Communities of Southern

577 Wisconsin. *Ecol. Monogr* 27:325–349. DOI: 10.2307/1942268.

578 Buck KR, Bentham WN. 1998. A novel symbiosis between a cyanobacterium, Synechococcus sp.,

579 an aplastidic protist, Solenicola setigera, and a diatom, Leptocylindrus mediterraneus, in

580 the open ocean. *Mar. Biol* 132:349–355. DOI: 10.1007/s002270050401.

581 Cael BB, Dutkiewicz S, Henson S. 2021. Abrupt shifts in 21st-century plankton communities.

582 *Science Advances* 7:eabf8593. DOI: 10.1126/sciadv.abf8593.

583 Campbell L, Vaulot D. 1993. Photosynthetic picoplankton community structure in the

584 subtropical North Pacific Ocean near Hawaii (station ALOHA. *Deep. Res. Part I:*

585 *Oceanographic Research Papers* 40:2043–2060. DOI: 10.1016/0967-0637(93)90044-4.

586 Capone DG, Hutchins DA. 2013. Microbial biogeochemistry of coastal upwelling regimes in a

587 changing ocean. *Nature Geoscience* 6:711–717. DOI: 10.1038/ngeo1916.

588 Carreto JI, Seguel M, Montoya NG, Clément A, Carignan MO. 2001. Pigment profile of the

589 ichthyotoxic dinoflagellate Gymnodinium sp. from a massive bloom in southern Chile. *J.*

590 *Plankton Res* 23:1171–1175.

591 Catlett D, Siegel DA, Simons RD, Guillocheau N, Henderikx-Freitas F, Thomas CS. 2021.

592 Diagnosing seasonal to multi-decadal phytoplankton group dynamics in a highly

593 productive coastal ecosystem. *Progress in Oceanography* 197:102637. DOI:

594 10.1016/j.pocean.2021.102637.

595   Chavez FP, Messié M, Pennington JT. 2011. Marine Primary Production in Relation to Climate

596   Variability and Change. *Annual Review of Marine Science* 3:227–260. DOI:

597   10.1146/annurev.marine.010908.163917.

598   Clarke KR. 1993. Non-parametric multivariate analyses of changes in community structure.

599   *Aust. J. Ecol* 18:117–143. DOI: 10.1111/j.1442-9993.1993.tb00438.x.

600   Clarke KR, Gorley RN, Somerfield PJ, Warwick RM. 2014. *Change in marine communities: an*

601   *approach to statistical analysis and interpretation*. PRIMER-E: Plymouth.

602   Claustre H. 1994. The trophic status of various oceanic provinces as revealed by phytoplankton

603   pigment signatures. *Limnology and Oceanography* 39. DOI: 10.4319/lo.1994.39.5.1206.

604   Clayton S, Gibala-Smith L, Mogatas K, Flores-Vargas C, Marciniak K, Wigginton M, Mulholland

605   MR. 2022. Imaging Technologies Build Capacity and Accessibility in Phytoplankton

606   Species Identification Expertise for Research and Monitoring: Lessons Learned During

607   the COVID-19 Pandemic. *Frontiers in Microbiology* 13:823109. DOI:

608   10.3389/fmicb.2022.823109.

609   Closset I, McNair HM, Brzezinski MA, Krause JW, Thamatrakoln K, Jones JL. 2021. Diatom

610   response to alterations in upwelling and nutrient dynamics associated with climate

611   forcing in the California Current System. *Limnology and Oceanography* 66:1578–1593.

612   DOI: https://doi.org/10.1002/lno.11705.

613   Drew LW. 2011. Are We Losing the Science of Taxonomy?: As need grows, numbers and training

614   are failing to keep up. *BioScience* 61:942–946. DOI: 10.1525/bio.2011.61.12.4.

615   Du X, Peterson WT. 2018. Phytoplankton Community Structure in 2011–2013 Compared to the

616   Extratropical Warming Event of 2014–2015. *Geophysical Research Letters* 45:1534–

617   1540. DOI: 10.1002/2017GL076199.

618   Du X, Peterson W, O'Higgins L. 2015. Interannual variations in phytoplankton community

619   structure in the northern California Current during the upwelling seasons of 2001-2010.

620   *Marine Ecology Progress Series* 519:75–87. DOI: 10.3354/meps11097.

621   Durkin CA, Cetinić I, Estapa M, Ljubešić Z, Mucko M, Neeley A, Omand M. 2022. Tracing the

622   path of carbon export in the ocean though DNA sequencing of individual sinking

623   particles. *The ISME Journal* 16:1896–1906. DOI: 10.1038/s41396-022-01239-2.

624   Fender CK, Kelly TB, Guidi L, Ohman MD, Smith MC, Stukel MR. 2019. Investigating Particle Size-

625   Flux Relationships and the Biological Pump Across a Range of Plankton Ecosystem States

626   From Coastal to Oligotrophic. *Frontiers in Marine Science* 6:603. DOI:

627   10.3389/fmars.2019.00603.

628   Finkel ZV, Sebbo J, Feist-Burkhardt S, Irwin AJ, Katz ME, Schofield OME, Young JR, Falkowski PG.

629   2007. A universal driver of macroevolutionary change in the size of marine

630   phytoplankton over the Cenozoic. 104:20416–20420. DOI: 10.1073/pnas.0709381104.

631   Finlay BJ. 2002. Global dispersal of free-living microbial eukaryote species. *Science* 296:1061–

632   1063. DOI: 10.1126/science.1070710.

633   Fischer AD, Hayashi K, McGaraghan A, Kudela RM. 2020. Return of the "age of dinoflagellates"

634   in Monterey Bay: Drivers of dinoflagellate dominance examined using automated

635   imaging flow cytometry and long-term time series analysis. *Limnology and*

636   *Oceanography* 65:2125–2141. DOI: 10.1002/lno.11443.

637 Fujiki T, Sasaoka K, Matsumoto K, Wakita M, Mino Y. 2016. Seasonal variability of

638   phytoplankton community structure in the subtropical western North Pacific. *Journal of*

639   *Oceanography* 72:343–358. DOI: 10.1007/s10872-015-0346-9.

640 Gómez F. 2007. The consortium of the protozoan Solenicola setigera and the diatom

641   Leptocylindrus mediterraneus in the Pacific Ocean. *Acta Protozool* 46:15–24.

642 Gorocs Z, Tamamitsu M, Bianco V, Wolf P, Roy S, Shindo K, Yanny K, Wu Y, Koydemir HC,

643   Rivenson Y, Ozcan A. 2018. A deep learning-enabled portable imaging flow cytometer

644   for cost-effective, high-throughput, and label-free analysis of natural water samples.

645   *Light-Science & Applications* 7:66. DOI: 10.1038/s41377-018-0067-0.

646 Gran HH, Thompson TG. 1930. *The diatoms and the physical and chemical conditions of the sea*

647   *water of the San Juan Archipelago*. University of Washington.

648 Hasle GR. 2002. Are most of the domoic acid-producing species of the diatom genus Pseudo-

649   nitzschia cosmopolites? *Harmful Algae* 1:137–146. DOI: https://doi.org/10.1016/S1568-

650   9883(02)00014-8.

651 Havskum H, Schluter L, Scharek R, Berdalet E, Jacquet S. 2004. Routine quantification of

652   phytoplankton groups-microscopy or pigment analyses? *Marine Ecology Progress Series*

653   273:31–42. DOI: 10.3354/meps273031.

654 Hickey B, Banas N. 2008. Why is the Northern End of the California Current System So

655   Productive? *Oceanography* 21:90–107. DOI: 10.5670/oceanog.2008.07.

656 Higgins HW, Wright SW, Schluter L. 2011. Quantitative interpretation of chemotaxonomic

657   pigment data. In: Roy S, Llewellyn CA, Egeland ES, Johansen AM eds. *Phytoplankton*

658   *Pigments: Characterization, Chemotaxonomy and Applications in Oceanography.*

659   Cambridge University Press, 257–313.

660   Hoepffner N, Haas LW. 1990. Electron microscopy of nanoplankton from the North Pacific

661   central gyre. *Journal of Phycology* 26:421–439. DOI: 10.1111/j.0022-3646.1990.00421.x.

662   Hooker SB, Clementson L, Thomas CS, Schlüter L, Allerup M, Ras J, Claustre H, Normandeau C,

663   Cullen J, Kienast M. 2012. The Fifth SeaWiFS HPLC Analysis Round-Robin Experiment

664   (SeaHARRE–5. In: *NASA Technical Memorandum 2012–217503*. Greenbelt, MD: NASA

665   Goddard Space Flight Center,.

666   Hoving H-J, Christiansen S, Fabrizius E, Hauss H, Kiko R, Linke P, Neitzel P, Piatkowski U,

667   Koertzinger A. 2019. The Pelagic In situ Observation System (PELAGIOS) to reveal

668   biodiversity, behavior, and ecology of elusive oceanic fauna. *Ocean Science* 15:1327–

669   1340. DOI: 10.5194/os-15-1327-2019.

670   Iriarte JL, Fryxell GA. 1995. Micro-phytoplankton at the equatorial Pacific (140°W) during the

671   JGOFS EqPac Time Series studies: March to April and October 1992. *Deep Sea Research*

672   *Part II: Topical Studies in Oceanography* 42:559–583. DOI:

673   https://doi.org/10.1016/0967-0645(95)00031-K.

674   Irigoien X, Meyer B, Harris R, Harbour D. 2004. Using HPLC pigment analysis to investigate

675   phytoplankton taxonomy: the importance of knowing your species. *Helgoland Marine*

676   *Research* 58:77–82. DOI: 10.1007/s10152-004-0171-9.

677   Kammerer JC. 1987. Largest Rivers in the United States (Water Fact Sheet. *US Geological Survey*

678   *Fact Sheet OFR*:87–242. DOI: 10.3133/OFR87242.

679   Karl DM, Church. MJ. 2017. Ecosystem Structure and Dynamics in the North Pacific Subtropical

680   Gyre: New Views of an Old Ocean. *Ecosystem* 20:433–457. DOI: 10.1007/s10021-017-

681   0117-0.

682   Kavanaugh MT, Church MJ, Davis CO, Karl DM, Letelier RM, Doney SC. 2018. ALOHA From the

683   Edge: Reconciling Three Decades of in Situ Eulerian Observations and Geographic

684   Variability in the North Pacific Subtropical Gyre. *Frontiers in Marine Science* 5:130. DOI:

685   10.3389/fmars.2018.00130.

686   Kodama T, Watanabe T, Taniuchi Y, Kuwata. A, Hasegawa. D. 2021. Micro-size plankton

687   abundance and assemblages in the western North Pacific Subtropical Gyre under

688   microscopic observation. *PLoS ONE* 16:0250604. DOI: 10.1371/journal.pone.0250604.

689   Kramer SJ, Siegel DA, Graff JR. 2020. Phytoplankton Community Composition Determined From

690   Co-variability Among Phytoplankton Pigments From the NAAMES Field Campaign.

691   *Frontiers in Marine Science* 7. DOI: 10.3389/fmars.2020.00215.

692   Kramer SJ, Siegel DA, Maritorena S, Catlett D. 2022. Modeling surface ocean phytoplankton

693   pigments from hyperspectral remote sensing reflectance on global scales. *Remote*

694   *Sensing of Environment* 270:112879. DOI: 10.1016/j.rse.2021.112879.

695   Kudela RM, Horner-Devine AR, Banas NS, Hickey BM, Peterson TD, McCabe RM, Lessard EJ,

696   Frame E, Bruland KW, Jay DA, Peterson JO, Peterson WT, Kosro PM, Palacios SL, Lohan

697   MC, Dever EP. 2010. Multiple trophic levels fueled by recirculation in the Columbia River

698   plume. *Geophys. Res. Lett* 37:1–7. DOI: 10.1029/2010GL044342.

699   Landry MR. 2003. Phytoplankton growth and microzooplankton grazing in high-nutrient, low-

700   chlorophyll waters of the equatorial Pacific: Community and taxon-specific rate

701 assessments from pigment and flow cytometric analyses. *J. Geophys. Res* 108. DOI:

702 10.1029/2000JC000744.

703 Legendre L, Le Fèvre J. 1995. Microbial food webs and the export of biogenic carbon in oceans.

704 *Aquatic Microbial Ecology* 9:69–77. DOI: 10.3354/ame009069.

705 Li WK. 1995. Composition of ultraphytoplankton in the central north Atlantic. *Mar. Ecol. Prog.*

706 *Ser* 122:1–8. DOI: 10.3354/MEPS122001.

707 Li B, Karl DM, Letelier RM, Bidigare RR, Church MJ. 2013. Variability of chromophytic

708 phytoplankton in the North Pacific Subtropical Gyre. *Deep. Res. Part II Top. Stud.*

709 *Oceanogr* 93:84–95. DOI: 10.1016/j.dsr2.2013.03.007.

710 Litchman E, Klausmeier CA, Schofield OM, Falkowski PG. 2007. The role of functional traits and

711 trade-offs in structuring phytoplankton communities: scaling from cellular to ecosystem

712 level. *Ecology Letters* 10:1170–1181. DOI: 10.1111/j.1461-0248.2007.01117.x.

713 Litzow MA, Hunsicker ME, Bond NA, Burke BJ, Cunningham CJ, Gosselin JL, Norton EL, Ward EJ,

714 Zador SG. 2020. The changing physical and ecological meanings of North Pacific Ocean

715 climate indices. *Proceedings of the National Academy of Sciences of the United States of*

716 *America* 117:7665–7671. DOI: 10.1073/pnas.1921266117.

717 Martiny JBH, Bohannan BJM, Brown JH, Colwell RK, Fuhrman JA, Green JL, Horner-Devine MC,

718 Kane M, Krumins JA, Kuske CR, Morin PJ, Naeem S, Øvreås L, Reysenbach AL, Smith VH,

719 Staley JT. 2006. Microbial biogeography: Putting microorganisms on the map. *Nat. Rev.*

720 *Microbiol* 4:102–112.

721 McQuatters-Gollop A, Johns D, Bresnan E, Skinner J, Rombouts I, Stern R, Aubert A, Johansen

722 M, Bedford J, Knights A. 2017. From microscope to management: The critical value of

723   plankton taxonomy to marine policy and biodiversity conservation. *Marine Policy* 83:1–

724   10. DOI: 10.1016/j.marpol.2017.05.022.

725 Michaels AF, Silver MW. 1988. Primary production, sinking fluxes and the microbial food web.

726   *Deep Sea Research Part A. Oceanographic Research Papers* 35:473–490. DOI:

727   10.1016/0198-0149(88)90126-4.

728 Miranda-Alvarez C, González-Silvera A, Santamaría-del-Angel E, López Calderón J, Godínez VM,

729   Sánchez Velasco L, Hernández Walls R. 2020. Phytoplankton pigments and community

730   structure in the northeastern tropical pacific using HPLC-CHEMTAX analysis. *J. Oceanogr*

731   76:91–108. DOI: 10.1007/s10872-019-00528-3.

732 Mirasbekov Y, Abdimanova A, Sarkytbayev K, Samarkhanov K, Abilkas A, Potashnikova D, Arbuz

733   G, Issayev Z, Vorobjev IA, Malashenkov D, Barteneva NS. 2021. Combining Imaging Flow

734   Cytometry and Molecular Biological Methods to Reveal Presence of Potentially Toxic

735   Algae at the Ural River in Kazakhstan. *Frontiers in Marine Science* 8:680482. DOI:

736   10.3389/fmars.2021.680482.

737 Moore JK, Fu W, Primeau F, Britten GL, Lindsay K, Long M, Doney SC, Mahowald N, Hoffman F,

738   Randerson JT. 2018. Sustained climate warming drives declining marine biological

739   productivity. *Science* 359:1139–1143. DOI: 10.1126/science.aao6379.

740 Morgan CA, De Robertis A, Zabel RW. 2005. Columbia River plume fronts. I. Hydrography,

741   zooplankton distribution, and community composition. *Mar. Ecol. Prog. Ser* 299:19–31.

742   DOI: 10.3354/meps299019.

743   Okada H, Honjo S. 1973. The distribution of oceanic coccolithophorids in the Pacific. *Deep Sea*

744   *Research and Oceanographic Abstracts* 20:355–374. DOI: 10.1016/0011-7471(73)90059-

745   4.

746   Olson RJ, Sosik HM. 2007. A submersible imaging-in-flow instrument to analyze nano- and

747   microplankton: Imaging FlowCytobot. *Limnol. Oceanogr.: Methods* 5:195–203. DOI:

748   10.4319/lom.2007.5.195.

749   Orr MC, Ferrari RR, Hughes AC, Chen J, Ascher JS, Yan Y-H, Williams PH, Zhou X, Bai M, Rudoy A,

750   Zhang F, Ma K-P, Zhu C-D. 2021. Taxonomy must engage with new technologies and

751   evolve to face future challenges. *Nature Ecology & Evolution* 5:3–4. DOI:

752   10.1038/s41559-020-01360-5.

753   Otero J, Álvarez-Salgado XA, Bode A. 2020. Phytoplankton Diversity Effect on Ecosystem

754   Functioning in a Coastal Upwelling System. *Frontiers in Marine Science* 7:592255. DOI:

755   10.3389/fmars.2020.592255.

756   Pal R, Choudhury AK. 2014. *An Introduction to Phytoplanktons: Diversity and Ecology*. Springer

757   New Delhi.

758   Pan H, Li A, Cui Z, Ding D, Qu K, Zheng Y, Lu L, Jiang T, Jiang T. 2020. A comparative study of

759   phytoplankton community structure and biomass determined by HPLC-CHEMTAX and

760   microscopic methods during summer and autumn in the central Bohai Sea, China.

761   *Marine Pollution Bulletin* 155:111172. DOI: 10.1016/j.marpolbul.2020.111172.

762   Parsons ML, Dortch Q. 2002. Sedimentological evidence of an increase in Pseudo-nitzschia

763   (Bacillariophyceae) abundance in response to coastal eutrophication. *Limnol. Oceanogr*

764   47:551–558. DOI: 10.4319/lo.2002.47.2.0551.

765   Partensky F, Blanchot J, Vaulot D. Differential distribution and ecology of Prochlorococcus and

766   Synechococcus in oceanic waters: a review. *Bull. l'Institut Oceanogr. Monaco*

767   1999b:457–475.

768   Partensky F, Hess WR, Vaulot D. Prochlorococcus, a Marine Photosynthetic Prokaryote of Global

769   Significance. *Microbiol. Mol. Biol. Rev* 1999a, 63:106–127.

770   Pearson DL, Hamilton AL, Erwin TL. 2011. Recovery Plan for the Endangered Taxonomy

771   Profession. *BioScience* 61:58–63. DOI: 10.1525/bio.2011.61.1.11.

772   Peterson W, Bond N, Robert M. 2016. The Blob (Part Three): Going, going, gone? - ProQuest.

773   *PICES Press* 24:46–48.

774   Picheral M, Guidi L, Stemmann L, Karl DM, Iddaoud G, Gorsky G. 2010. The Underwater Vision

775   Profiler 5: An advanced instrument for high spatial resolution studies of particle size

776   spectra and zooplankton. *Limnol. Oceanogr.: Methods* 8:462–473.

777   Pomeroy L. 1974. Oceans Food Web, a Changing Paradigm. *Bioscience* 24:499–504. DOI:

778   10.2307/1296885.

779   Ramond P, Siano R, Schmitt S, deVargas C, Marié L, Memery. L, Sourisseau M. 2021.

780   Phytoplankton taxonomic and functional diversity patterns across a coastal tidal front.

781   *Sci Rep* 11:2682. DOI: 10.1038/s41598-021-82071-0.

782   Reid FMH. 1980. Coccolithophorids of the North Pacific Central Gyre with Notes on Their

783   Vertical and Seasonal Distribution. *Micropaleontology* 26:151–176. DOI:

784   10.2307/1485436.

785 Rost B, Zondervan I, Wolf-Gladrow D. 2008. Sensitivity of phytoplankton to future changes in

786   ocean carbonate chemistry: current knowledge, contradictions and research directions.

787   *Marine Ecology Progress Series* 373:227–237. DOI: 10.3354/meps07776.

788 Roy S, Llewellyn CA, Egeland ES, Pigments JGP. 2011. *Characterization, Chemotaxonomy and*

789   *Applications in Oceanography*. Cambridge University Press.

790 Sherr EB, Sherr BF. 1991. Planktonic microbes: Tiny cells at the base of the ocean's food webs.

791   *Trends in Ecology & Evolution* 6:50–54. DOI: 10.1016/0169-5347(91)90122-E.

792 Shin H, Lee E, Shin J, Ko S-R, Oh H-S, Ahn C-Y, Oh H-M, Cho B-K, Cho S. 2018. Elucidation of the

793   bacterial communities associated with the harmful microalgae Alexandrium tamarense

794   and Cochlodinium polykrikoides using nanopore sequencing. *Scientific Reports* 8:5323.

795   DOI: 10.1038/s41598-018-23634-6.

796 Smith JC, Cormier R, Worms J, Bird CJ, Quilliam MA, Pocklington R, Angus R, Hanic L. 1990. Toxic

797   Blooms of the Domoic Acid Containing Diatom Nitzschia pungens in the Cardigan River,

798   Prince Edward Island, in 1988. In: *Toxic Mar. Phytoplankt*. Elsevier, 227–232.

799 Steele JH, Thorpe SA, Turekian KK. 2008. *Encyclopedia Of Ocean Sciences*. Academic Press.

800 Šupraha L, Ljubešić Z, Henderiks J. 2018. Combination coccospheres from the Eastern Adriatic

801   coast: New, verified and possible life-cycle associations. *Marine Micropaleontology*

802   141:23–30. DOI: 10.1016/j.marmicro.2018.04.001.

803 Taylor A, Landry M. 2018. Phytoplankton biomass and size structure across trophic gradients in

804   the southern California Current and adjacent ocean ecosystems. *Marine Ecology*

805   *Progress Series* 592:1–17. DOI: 10.3354/meps12526.

806   Thomas MK, Kremer CT, Klausmeier CA, E L. 2012. A global pattern of thermal adaptation in

807   marine phytoplankton. *Science* 338:1085–1088. DOI: 10.1126/science.1224836.

808   Thomsen HA, Buck KR, Marino D, Sarno D, Hansen LE, Osergaard JB, Krupp J. 1993. Lennoxia

809   faveolata, new genus new species (Diatomophyceae) from South America, California,

810   West Greenland and Denmark. *Phycologia* 32:278–283.

811   Trainer VL, Adams NG, Bill BD, Stehr CM, Wekell JC, Moeller P, Busman M, Woodruff D. 1998.

812   Domoic acid production near California coastal upwelling zones. *Oceanogr* 45:1818–

813   1833. DOI: 10.4319/lo.2000.45.8.1818.

814   Trainer VL, Bates SS, Lundholm N, Thessen AE, Cochlan WP, Adams NG, Trick CG. 2012. Pseudo-

815   nitzschia physiological ecology, phylogeny, toxicity, monitoring and impacts on

816   ecosystem health. *Harmful Algae* 14:271–300. DOI: 10.1016/j.hal.2011.10.025.

817   Utermöhl H. 1958. Zur Vervollkommnung der quantitativen Phytoplankton-Methodik (Towards

818   a perfection of quantitative phytoplankton methodology. *Mitt. int. Ver. theor. angew.*

819   *Limnol* 9:1–38. DOI: 10.1080/05384680.1958.11904091.

820   Vandermeulen RA, Mannino A, Craig SE, Werdell PJ. 2020. 150 shades of green: Using the full

821   spectrum of remote sensing reflectance to elucidate color shifts in the ocean. *Remote*

822   *Sensing of Environment* 247:111900. DOI: 10.1016/j.rse.2020.111900.

823   Venrick EL. 1971. Recurrent Groups of Diatom Species in the North Pacific. *Ecology* 52:614–625.

824   DOI: 10.2307/1934149.

825   Venrick EL. 1990. Phytoplankton in an Oligotrophic Ocean: Species Structure and Interannual

826   Variability. *Ecology* 71:1547–1563. DOI: 10.2307/1938291.

827   Venrick EL, McGowan JA, Cayan DR, Hayward TL. 1987. Climate and Chlorophyll a: Long-Term

828   Trends in the Central North Pacific Ocean. *Science* 238:70–72. DOI:

829   10.1126/science.238.4823.7.

830   Villarino E, Watson JR, Jönsson B, Gasol JM, Salazar G, Acinas SG, Estrada M, Massana R,

831   Logares R, Giner CR, Pernice MC, Olivar MP, Citores L, Corell J, Rodríguez-Ezpeleta N,

832   Acuña JL, Molina-Ramírez A, González-Gordillo JI, Cózar A, Martí E, Cuesta JA, Agustí S,

833   Fraile-Nuez E, Duarte CM, Irigoien X, Chust. G. 2018. Large-scale ocean connectivity and

834   planktonic body size. *Nat. Commun* 9, 142. DOI: 10.1038/s41467-017-02535-8.

835   Volk T, Hoffert MI. 1985. Ocean Carbon Pumps: Analysis of Relative Strengths and Efficiencies in

836   Ocean-Driven Atmospheric CO2 Changes. In: *The Carbon Cycle and Atmospheric CO2:*

837   *Natural Variations Archean to Present*. American Geophysical Union (AGU), 99–110.

838   DOI: 10.1029/GM032p0099.

839   Ware DM, Thomson RE. 2005. Bottom-Up Ecosystem Trophic Dynamics Determine Fish

840   Production in the Northeast Pacific. *Science* 308:1280–1284. DOI:

841   10.1126/science.1109049.

842   Werdell PJ, Behrenfeld MJ, Bontempi PS, Boss E, Cairns B, Davis GT, Franz BA, Gliese UB,

843   Gorman ET, Hasekamp O, Knobelspiesse KD, Mannino A, Martins JV, McClain CR,

844   Meister G, Remer LA. 2019. The Plankton, Aerosol, Cloud, ocean Ecosystem (PACE)

845   mission: Status, science, advances. *Bull. Amer. Meteor. Soc* 100:1775-1794,. DOI:

846   10.1175/BAMS-D-18-0056.1.

847   Winder M, Sommer U. 2012. Phytoplankton response to a changing climate. *Hydrobiologia*

848   698:5–16. DOI: 10.1007/s10750-012-1149-2.

849 Yamaguchi A, Watanabe Y, Ishida H, Harimoto T, Furusawa K, Suzuki S, Ishizaka J, Ikeda T,

850   Takahashi MM. 2002. Structure and size distribution of plankton communities down to

851   the greater depths in the western North Pacific Ocean. *Deep Sea Research Part II:*

852   *Topical Studies in Oceanography* 49:5513–5529. DOI: 10.1016/S0967-0645(02)00205-9.

853 Yoon J-E, Kim I-N. 2020. Climate-driven phytoplankton community shifts in the North Pacific

854   Subtropical Gyre. In: *EGU General Assembly Conference Abstracts*. EGU General

855   Assembly Conference Abstracts. 6754.

856 Zhang Y, Wang X, Yin K. 2018. Spatial contrast in phytoplankton, bacteria and microzooplankton

857   grazing between the eutrophic Yellow Sea and the oligotrophic South China Sea. *J.*

858   *Ocean. Limnol* 36:92–104. DOI: 10.1007/s00343-018-6259-x.

859

Figure 1

Investigation area superimposed on satellite data

Cruise track of the Sea to Space cruise (black line), showing approximate position of Station 1, Station 2, and Station 3, superimposed onto: a) MODIS Aqua Sea Surface temperature, b) MODIS Aqua Chlorophyll a concentration, and c) Apparent Visible Wavelength. All satellite data is monthly average for February 2017
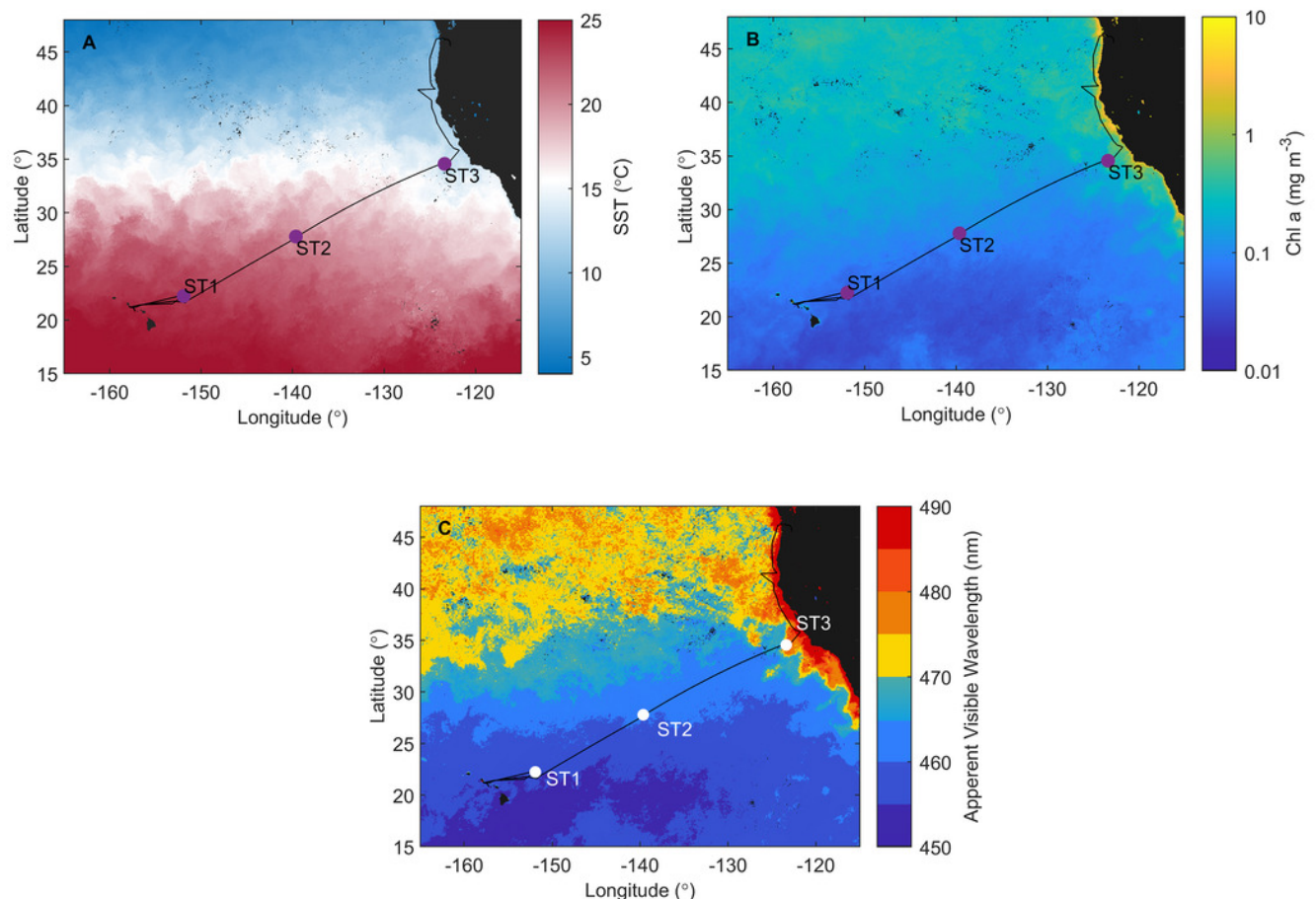
Figure 2

Spatial distribution of phytoplankton along the sampling transect in North Pacific

Spatial distribution of phytoplankton along the sampling transect in North Pacific: (a) microphytoplankton fraction; (b) nanophytoplankton fraction. Stations (Station 1, Station 2, and Station 3) with sampling sites as CTD casts and corresponding depth (the surface layer (S), deep chlorophyll maximum (DCM), and mixed layer depth (MLD)) are shown on x-axis. Abundances (cellsL1) of diatoms, dinoflagellates, coccolithophores, and others are shown on y
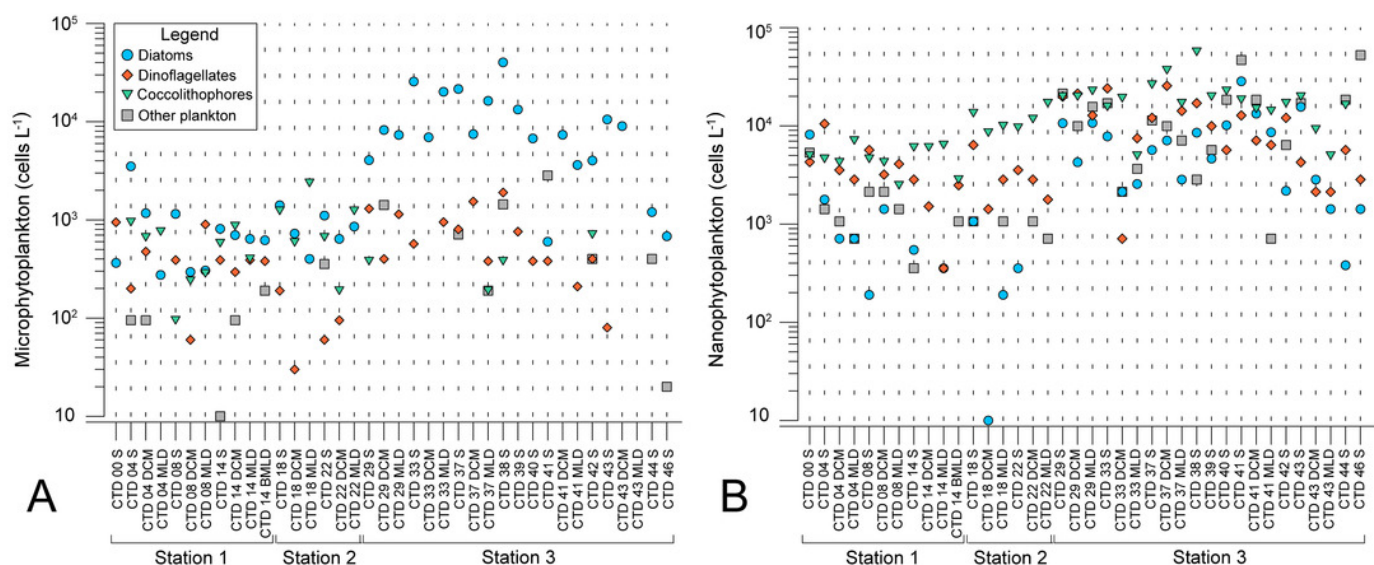
Figure 3

Spatial distribution of pigments along the sampling transect in North Pacific:

(a) Pigments that correlated the most with the phytoplankton abundances: alloxanthine, zeaxanthin, divinyl chlorophyll *a* (DVChl *a*), divinyl chlorophyll *b* (DVCHl *b*), and lutein. (b) Total chlorophyll *a* (Chl *a*). Stations (Station 1, Station 2, and Station 3) with sampling sites as CTD casts and corresponding depths (the surface layer (S), deep chlorophyll maximum (DCM), and mixed layer depth (MLD)) are shown on x-axis. Concentrations of pigments (μL^{-1}) are shown on y-axis (log-scale at (b))
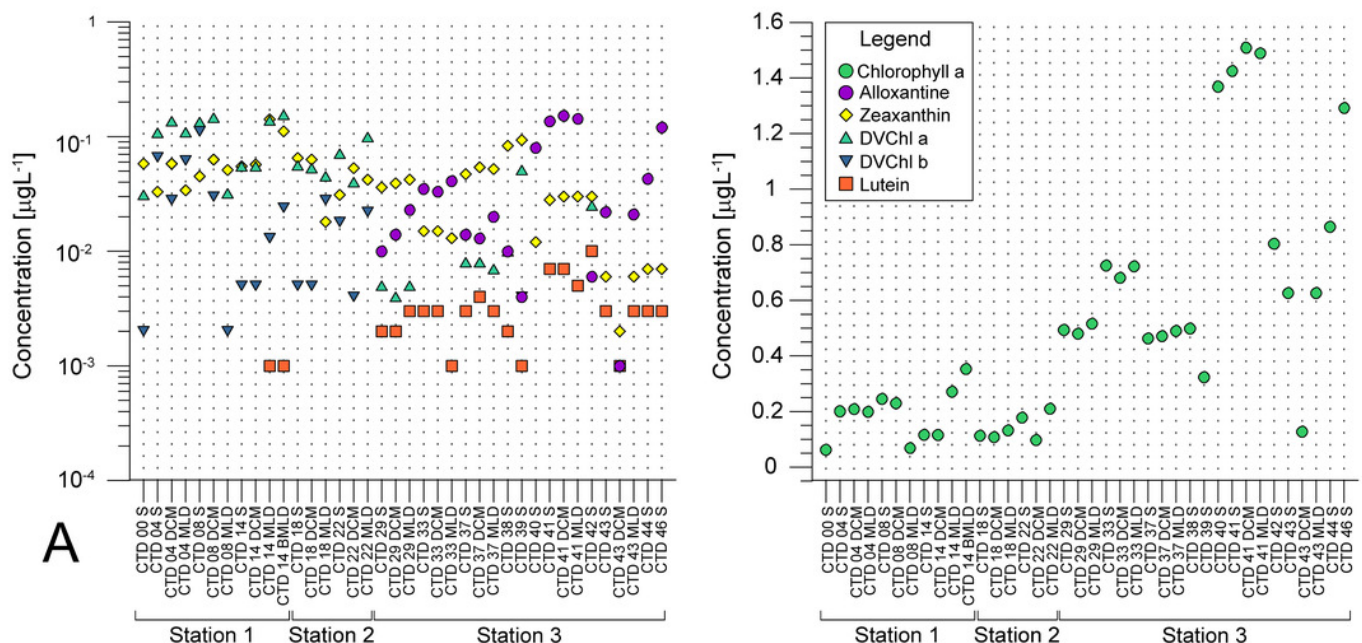
Figure 4

Micrographs of dominant species at Station 1 (ST1), Station 2 (ST2) and Station 3 (ST3).

Micrographs of dominant species at Station 1 (ST1), Station 2 (ST2) and Station 3 (ST3). From top left to bottom right: (A) Chaetoceros convolutus (ST3), (B) Rhizosolenia clevei with Richelia intracelularis (arrow, ST3), (C) Nitzschia longissima (ST1), (D) Thalassiosira sp. (ST3), (E) Ophiaster sp. (ST2), (F) Cryptophyta (ST3), (G) Phytoflagellates (ST1), (H) Chaetoceros debilis (ST3), (I) Thalassionema nitzschioides (ST3), (J) Michaelsarsia adriaticus (ST1), (K) Nitzschia bicapitata (ST3), (L) Discosphaera tubifera (ST2)
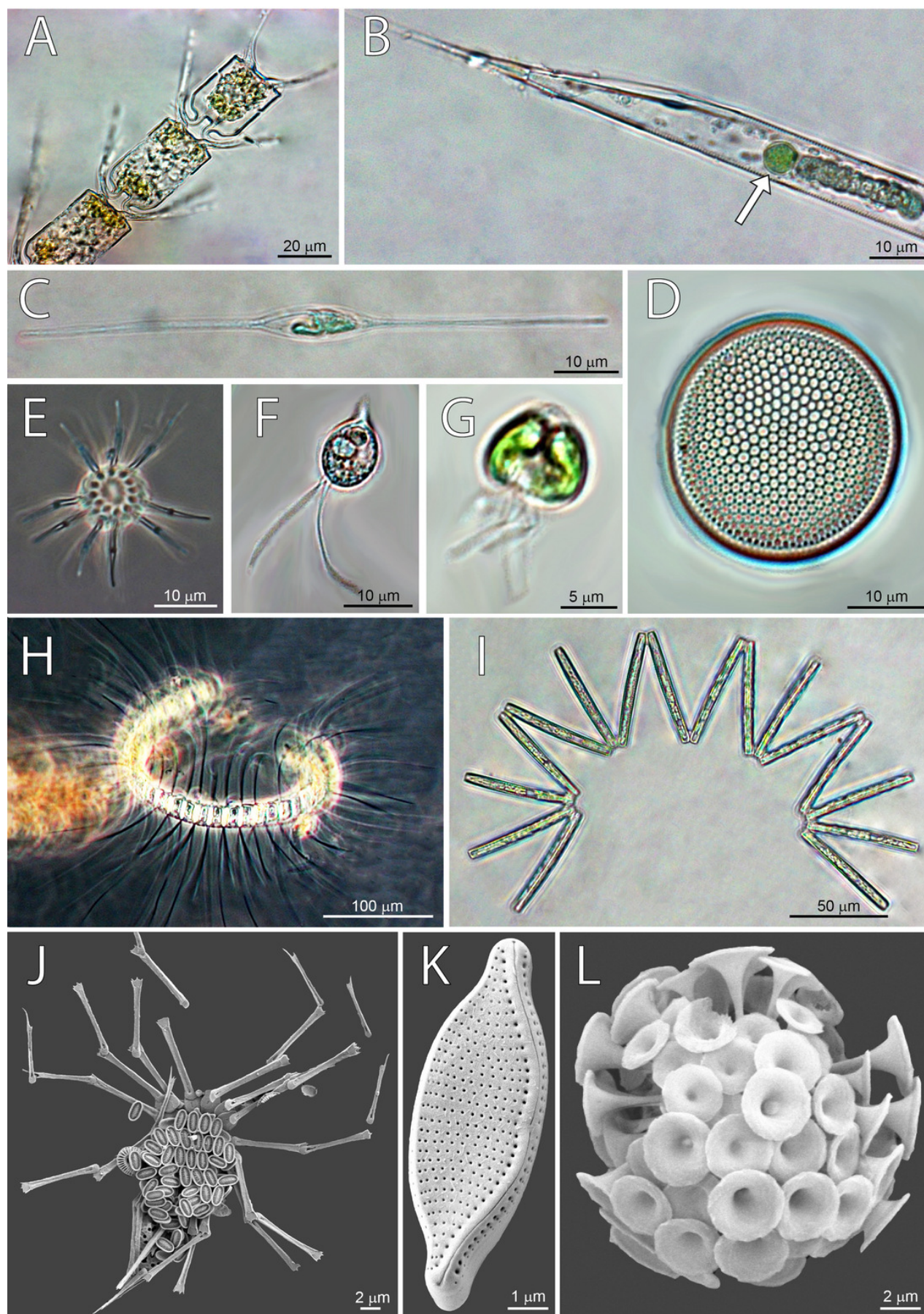
Figure 5

LINKTREE binary divisive clustering analysis of the phytoplankton community at 37 sites.

Each split is constrained by a threshold of one of four best correlated pigments: alloxanthin (Allo), zeaxanthin (Zea), divinyl Chl b (DVChl b), and lutein (Lut). The first in-equality indicates sites to the left side of the split, the second sites to the right. The primary split is marked with A. Clusters marked with red dotted line are not significant by SIMPROF test. Split results: A->B,K Allo < -8,89E+03 (>0,001); B->C Lut < -8,89E+03 (>0,001) or Zea <0,065 (>0,111); K->L,N Zea <0,007 (>0,012); N->O Lut <0,007 (>0,01)
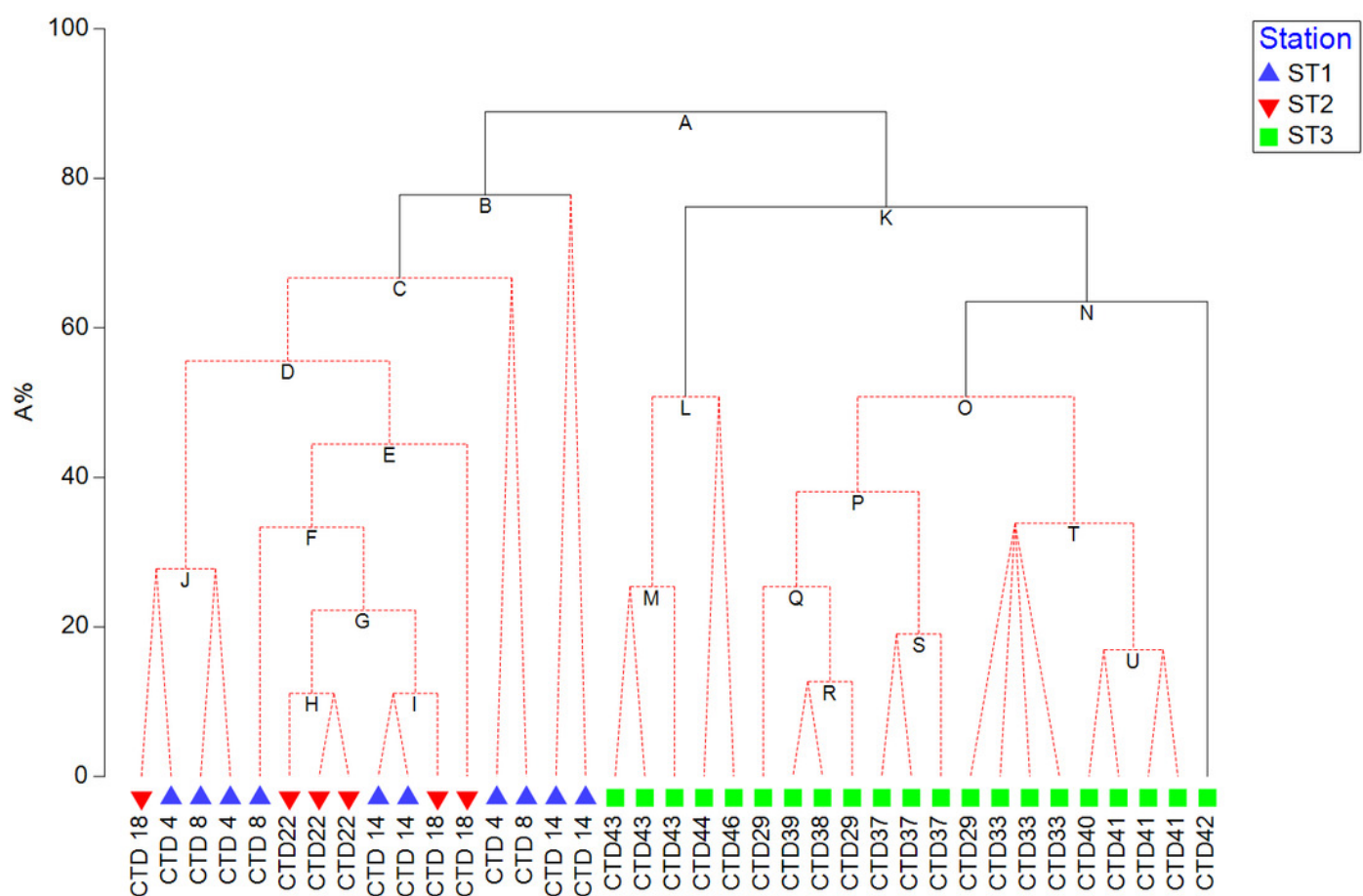
Sampling sites within each station: Station 1 (ST1), Station 2 (ST2), and Station 3 (ST3).

CTD casts, corresponding depths and water column layers are shown for each site, as well as which sample type is taken (+). Abbreviations: PHYTO (samples taken for light microscopy and pigment analyses); SEM (samples taken for scanning electron microscopy); NET (samples taken with phytoplankton net with 20μm mash size).

1 **Table 1.** Sampling sites within each station: Station 1 (ST1), Station 2 (ST2), and Station 3 (ST3). Total number of
2 samples (N)=103, of which N=25 at ST1, N=22 at ST2, and N=56 at ST3. CTD casts, corresponding depths and water
3 column layers are shown for each site, as well as which sample type is taken (+). Abbreviations: PHYTO (samples
4 (N=38) taken for light microscopy and pigment analyses); SEM (samples (N=38) taken for scanning electron
5 microscopy); NET (samples (N=27) taken with phytoplankton net with 20 μm mash size).

Station	Sampling site (latitude; longitude)	CTD Cast	Depth	Water column layer	PHYTO	SEM	NET
Station 1	22°14.6892; -151°52.2906	CTD4	0	S	+	+	
		CTD4	115	DCM	+	+	
		CTD4	130	MLD	+	+	
	22°16.5251; -151°44.8940	CTD8	0	S	+	+	
		CTD8	115	DCM	+	+	
		CTD8	125	MLD	+	+	+
	22°16.5251; -151°44.8940	CTD14	0	S	+	+	+
		CTD14	88	DCM	+	+	+
		CTD14	128	MLD	+	+	+
		CTD14	180	BMLD	+	+	+
Station 2	27°42.5971; -139°29.9381	CTD18	0	S	+	+	+
		CTD18	98	DCM	+	+	+
		CTD18	128	MLD	+	+	+
	27°39.6715; -139°33.0614	CTD19	130	MLD		+	
		CTD19	composite				+
	27°42.0327; -139°41.7295	CTD21	0	S	+	+	
	27°44.7694; -139°40.2311	CTD22	0	S	+	+	+
		CTD22	95	DCM	+	+	+
		CTD22	120	MLD	+	+	+
Station 3	34°34.1060; -123°30.6151	CTD29	0	S	+	+	
		CTD29	31	DCM	+	+	
		CTD29	42	MLD	+	+	
		CTD29	composite				+
	34°31.5869; -123°33.9840	CTD33	0	S	+	+	
		CTD33	27	DCM	+	+	
		CTD33	30	MLD	+	+	
		CTD33	composite				+
	34°18.2352; -123°32.4584	CTD37	0	S	+	+	
		CTD37	2	DCM	+	+	
		CTD37	38	MLD	+	+	
		CTD37	composite				+
	34°30.011; -123°11.1985	CTD38	0	S	+	+	+
	34°54.3259; -122°41.4444	CTD39	0	S	+	+	+
	35°40.1678; -121°55.7237	CTD40	0	S	+	+	+
	35°58.2849; -122°13.5212	CTD41	0	S	+	+	+

	CTD41	14	DCM	+		
	CTD41	27	MLD	+	+	
	CTD41	composite				+
41°28.4439; -126°18.8841	CTD42	0	S	+	+	+
	CTD43	0	S	+	+	+
41°30.6406; -125°20.7072	CTD43	80	DCM	+	+	+
	CTD43	90	MLD	+	+	+
	CTD43	composite				+
41°32.8395; -124°24.2721	CTD44	0	S	+	+	+
41°32.8395; -124°24.2722	CTD46	0	S	+	+	+

Similarities percentage (SIMPER) analysis for each taxon/group by stations.

Similarities percentage (SIMPER) analysis for each taxon/group by stations ST1, ST2, and ST3. Analyses was done on samples for light microscopy (N=38) and net phytoplankton samples (N=27), of which N=15 at ST1, N=14 at ST2, and N=36 at ST3. . Blank cells are values that could not be determined because there were less than 40 cells in 1L. Taxa with similarity contribution < 2 have been excluded from this table. Abbreviations: average contribution/standard deviation (δ/σ), species contribution (Σδ%).

1 **Table 2.** Similarities percentage (SIMPER) analysis for each taxon/group by stations ST1, ST2, and ST3.
2 Analyses was done on samples for light microscopy (N=38) and net phytoplankton samples (N=27), of
3 which N=15 at ST1, N=14 at ST2, and N=36 at ST3. . Blank cells are values that could not be determined
4 because there were less than 40 cells in 1L. Taxa with similarity contribution < 2 have been excluded
5 from this table. Abbreviations: average contribution/standard deviation (δ/σ), species contribution
6 (Σδ%).

Taxon/Group	Station 1 (δ/σ, Σδ%)	Station 2 (δ/σ, Σδ%)	Station 3 (δ/σ, Σδ%)
Undetermined dinoflagellates (10-20 μm)	5.44, 13.84	8.06, 12.37	1.64, 7.41
Undetermined coccolitophorids (<5 μm)	1.79, 12.09	6.72, 14.02	1.67, 7.81
Cryptophyceae	0.91, 5.75	1.02, 5.60	4.97, 9.02
Gyrodinium spp.	0.65, 2.50	0.70, 2.05	1.26, 4.02
Nitzschia bicapitata	0.52, 2.50	0.68, 2.45	0.65, 2.10
Chaetoceros perpusillus	0.61, 2.39	1.03, 3.22	
Undetermined dinoflagellates (5-10 μm)	0.91, 6.13	0.72, 4.30	
Leptocylindrus mediterraneus	0.66, 2.02	0.72, 2.05	
Undetermined coccolitophorids (5-10 μm)	8.47, 15.61		6.40, 10.06
Nitzschia longissimi	0.67, 2.33		2.17, 5.41
Phytoflagellates	1.24, 7.61		1.06, 4.63
Undetermined pennate diatoms (<20 μm)	0.53, 2.36		0.75, 3.16
Nitzschia sp.	0.67, 2.06		
Michelsarsia adriatica	0.63, 2.37		
Gyrodinium spp. (<20 μm)	0.53, 2.54		
Gymnodinium spp.	0.52, 2.67		
Undetermined coccolithophorids (10-20 μm)		7.43, 12.20	
Discosphaera tubifera		1.64, 6.67	
Calciosolenia murrayi		1.55, 5.87	
Calciosolenia brasiliensis		0.72, 2.99	
Rhizosolenia hebetata f. semispina		7.34, 14.73	1.60, 3.52
Pseudo-nitzschia pseudodelicatissima			6.14, 7.62
Chaetoceros convolutes			1.61, 4.93
Rhizosolenia cleveii			1.03, 2.68
Lennoxia faveolata			0.88, 3.84
Thalassiosira (<20 μm)			0.88, 3.83

Chaetoceros contortus	0.74, 2.21

Maximum abundances (cells L-1), and frequencies (%) for dominant species at Station 1 (ST1), Station 2 (ST2) and Station 3 (ST3).

Maximum abundances (cells L^{-1}), and frequencies (%) for dominant species (where dominance is defined as frequency of appearance in samples >50 %) at Station 1 (ST1), Station 2 (ST2) and Station 3 (ST3). Total number of samples (N)=103, of which N=25 at ST1, N=22 at ST2, and N=56 at ST3. Blank cells are values that could not be determined because there were less than 40 cells in 1 L.

1 **Table 3.** Maximum abundances (cells L^{-1}), and frequencies (%) for dominant species (where dominance is
2 defined as frequency of appearance in samples >50 %) at Station 1 (ST1), Station 2 (ST2) and Station 3
3 (ST3). Total number of samples (N)=103, of which N=25 at ST1, N=22 at ST2, and N=56 at ST3. Blank cells
4 are values that could not be determined because there were less than 40 cells in 1 L.

Dominant Taxa/Group	Max (ST1)	Fr (ST1)	Max (ST2)	Fr (ST2)	Max (ST3)	Fr (ST3)
Chaetoceros contortus					2660	63
Chaetoceros convolutus					5320	88
Chaetoceros debilis					2660	50
Chaetoceros perpusillus	380	60	380	75		
Lennoxia faveolata					14200	69
Leptocylindrus mediterraneus	190	60	380	63		
Nitzschia bicapitata	710	50	1420	63	4260	56
Nitzschia braarudii	190	50				
Nitzschia longissima	285	60			3800	94
Nitzschia sicula					760	50
Nitzschia sp.	570	60				
Nitzschia sp. 1			285	50		
Proboscia alata					380	50
Pseudo-nitzschia pseudodelicatissima					22420	100
Rhizosolenia hebetata f. semispina					1900	88
Rhizosolenia cleveii					1140	75
Thalassionema nitzschioides					1900	50
Thalassiosira sp. (<20 µm)					8520	69
Unknown diatoms (<20 µm)	1420	50			10650	63
Gymnodinium spp.	380	50				
Gyrodinium spp.	710	60	190	63	1140	81
Gyrodinium spp. (<20 µm)	3550	50				
Oxytoxum cf. variabile (<20 µm)					2130	50
N.D. dinoflagellates (5-10 µm)	1420	70	2130	63	19880	50
N.D. dinoflagellates (10-20 µm)	2840	100	4615	100	19880	88
Calciosolenia brasiliensis			380	63		
Calciosolenia murrayi	570	50	760	88		
Discosphaera tubifera	570	50	760	88		
Michaelsarsia adriaticus	190	60				
Ophiaster sp.			950	50		
N.D. coccolithophorids (<5µm)	3550	90	7810	100	24140	88
N.D. coccolithophorids (5-10 µm)	4615	100	8520	100	29820	100
N.D. coccolithophorids (10 - 20 µm)			3195	100		
Cryptophyceae	1065	70	1065	75	32660	100
Micromonas sp.					2840	50
Phytoflagellates	1065	80			8520	75